Viologen–Cycloparaphenylene Hybrids: Luminescent Molecular Nanocarbons for Anion Binding and Specific Vapor Sorption

Supplementary Information

by Rafał Frydrych, Kabali Senthilkumar, Katarzyna Ślusarek, Mateusz Waliczek, Wojciech Bury, Piotr J. Chmielewski, Joanna Cybińska, and Marcin Stępień*

Table of Contents

1. General

1.1. Synthetic Methods

Tetrahydrofuran, toluene, 1,4-dioxane and N,N-Dimethylformamide were freeze-pump-thawed prior to use. All other solvents and reagents were used as received. Compounds **S1, S2, S3** and **3** were prepared according to modified literature procedures.[1] Recycling gel permeation chromatography (GPC) was carried out using an JAI LaboACE LC-7080 chromatograph equipped with a RID (RI-700 LA) and UV-Vis (UV-VIS4ch 800LA) detectors and a preparative GPC columns JAIGEL-2HR and JAIGEL-2.5HR (size 20.0 mm ID × 600 mm each) in series, using 20 mM solution of sodium trifluoroacetate in DMF with 0.2% TFA as an eluent with a flow rate of 10 mL/min at 50 °C.

1.2. Analytical Methods

^{1}H NMR spectra were recorded on high-field spectrometers (^{1}H frequency 500.13 or 600.13 MHz), equipped with broadband inverse or conventional gradient probeheads. Spectra were referenced to the residual solvent signals (chloroform-*d*, 7.26 ppm, DMSO-d_6, 2.50 ppm, acetonitrile-d_3, 1.94). Two-dimensional NMR spectra were recorded with 2048 data points in the t_2 domain and up to 2048 points in the t_1 domain, with a 1.5 s recovery delay. All 2D spectra were recorded with gradient selection. ^{13}C NMR spectra were recorded with ^{1}H broadband decoupling and referenced to solvent signals ($^{13}CDCl_3$, 77.0 ppm; $(^{13}CD_3)_2SO$, 39.5 ppm; $^{13}CD_3CN$, 1.3 ppm; $CD_3{}^{13}CN$, 118.3 ppm). High resolution mass spectra were recorded using ESI ionization in the positive mode on Bruker Apex ultra FT-ICR. Absorption spectrometry was performed using Agilent Cary 60 UV-vis spectrophotometer and PerkinElmer Lambda 1050+ UV-vis-NIR spectrophotometer.

Gas and Vapor Sorption Analyses. All gas and vapor sorption isotherms were measured on a Micromeritics ASAP 2020M surface area and porosimetry system. Prior to the measurements, the sample of **1** was degassed at 40 °C for 24 h. All measurements (*n*-hexane, cyclohexane, 2,3-dimethylbutane, water) were carried out at the temperature 293 K.

Excitation and emission spectra were obtained using a FLS980 spectrofluorimeter (Edinburgh Instruments Ltd.) equipped with a 450 W Xenon lamp excitation source and a red-sensitive photomultiplier (Hamamatsu R-928P) operating within 200–870 nm. The former spectra were corrected for the incident light intensity and the latter for the wavelength-dependence of the emission channel sensitivity. Quantum yields were measured using a cooled extended-red Hamamatsu photomultiplier operating in a range of 200 – 1050 nm. Quantum yield measurements were performed by using an Edinburgh Instruments integrating sphere equipped with a small elliptical mirror and a baffle plate for beam steering and shielding against directly detected light. For the measurement, the integrating sphere replaces the standard sample holder inside the sample chamber. Calculations of quantum yields were made using the software provided by Edinburgh Instruments. The luminescence decay traces were registered by means of F-G05PM featuring a Hamamatsu H5773-04 detector. As an excitation source picosecond pulsed light emitting diode 360 nm was used.

^{1}H NMR spectroscopic titration studies.[2,3] The receptor solutions of [**1**][TFA]$_2$ were titrated in an NMR tube sealed with a plastic stopper, by adding known quantities of a stock solution of either [**P**], [**PMS**$^-$][Na$^+$]$_2$ or [**TSP**$^{4-}$][Na$^+$] in the same solvent. These solutions contained compound [**1**][TFA]$_2$ to ensure a constant concentration of the guest throughout the titration. After each addition the NMR tube was quickly shaken to ensure good mixing of the solutions and after temperature stabilization the spectra were recorded. [**P**], [**PMS**$^-$][Na$^+$]$_2$ and [**TSP**$^{4-}$][Na$^+$] were purchased from Sigma–Aldrich. The fitting, performed with the Bindfit software,[4] takes into account all data sets at the same time, thus improving the quality of the non-linear curve fitting.

Electrochemical measurements were performed on an Autolab(Metrohm) potentiostat/galvanostat system using a glassy-carbon working electrode, platinum wire as the auxiliary electrode, and silver/silver chloride as a reference electrode. The voltammograms were referenced against the half-wave potential of Fc^+ /Fc.

1.3. Computational Methods

Density functional theory (DFT) calculations were performed using Gaussian 16.[5] DFT geometry optimizations were carried out in unconstrained C_1 symmetry, using molecular mechanics or semiempirical models as starting geometries. The calculations were performed using the hybrid functional B3LYP,[6–8] including the CAM[9] and GD3BJ[10] corrections, and the 6-31G(d,p) basis set. Wavefunctions were tested for instabilities and, if required, reoptimized until a stable solution was found. Each structure was optimized to meet standard convergence criteria. The existence of a local minimum was verified by a normal mode frequency calculation.

2. Synthesis and Characterization

4-((1'*s*,4'*s*)-4''-Chloro-1',4'-dimethoxy-1',4'-dihydro-[1,1':4',1''-terphenyl]-4-yl)pyridine (**4**)

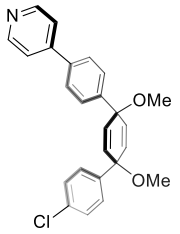

Compound **3** (3.000 g, 7.39 mmol, 1 equiv), phenylboronic acid (0.937 g, 0.84 mmol, 7.39 equiv), $Pd(PPh_3)_4$ (0.129 g, 0.111 mmol, 0.015 equiv), and K_2CO_3 (2.064 g, 14.8 mmol, 2 equiv) were dissolved in degassed 1,4-dioxane (15 mL) and water (3 ml) under argon atmosphere. The reaction mixture was stirred at 100 °C in MW (200 W), power max mode for 2 h, cooled down to room temperature, and added to water. The reaction mixture was then extracted with dichloromethane, combined organic layers were washed with brine, then dried over sodium sulfate, and evaporated under reduced pressure. The crude mixture was purified by using basic alumina column chromatography, gradient 20-70 % DCM in hexane solvent mixture, to get a pure product of compound 2 (40% yield).

^{1}H NMR (500 MHz, chloroform-*d*, 300 K): δ 8.63 (2H, d, *J* = 4.5 Hz), 7.57 (2H, d, *J* = 6.7 Hz), 7.47 (4H, d, *J* = 5.7 Hz), 7.42 (0.5, d, *J* = 8.7 Hz), 7.33 (1.5H, d, *J* = 6.6 Hz), 7.26 (2H, d, *J* = 6.6 Hz), 6.10 (4H, d, *J* = 16.5 Hz), 3.43 (3H, s), 3.41 (3H, s).

^{13}C NMR (125 MHz, chloroform-*d*, 300 K): δ 150.26, 147.74, 144.25, 142.40, 141.87, 137.44, 133.42, 133.36, 131.47, 128.52, 127.79, 127.44, 127.03, 126.72, 121.51, 74.60, 74.40, 52.04, 52.02.

HRMS (ESI–TOF): *m/z*: $[M + H]^+$ Calcd for $C_{25}H_{22}ClNO_2$: 404.1412; Found 404.1385.

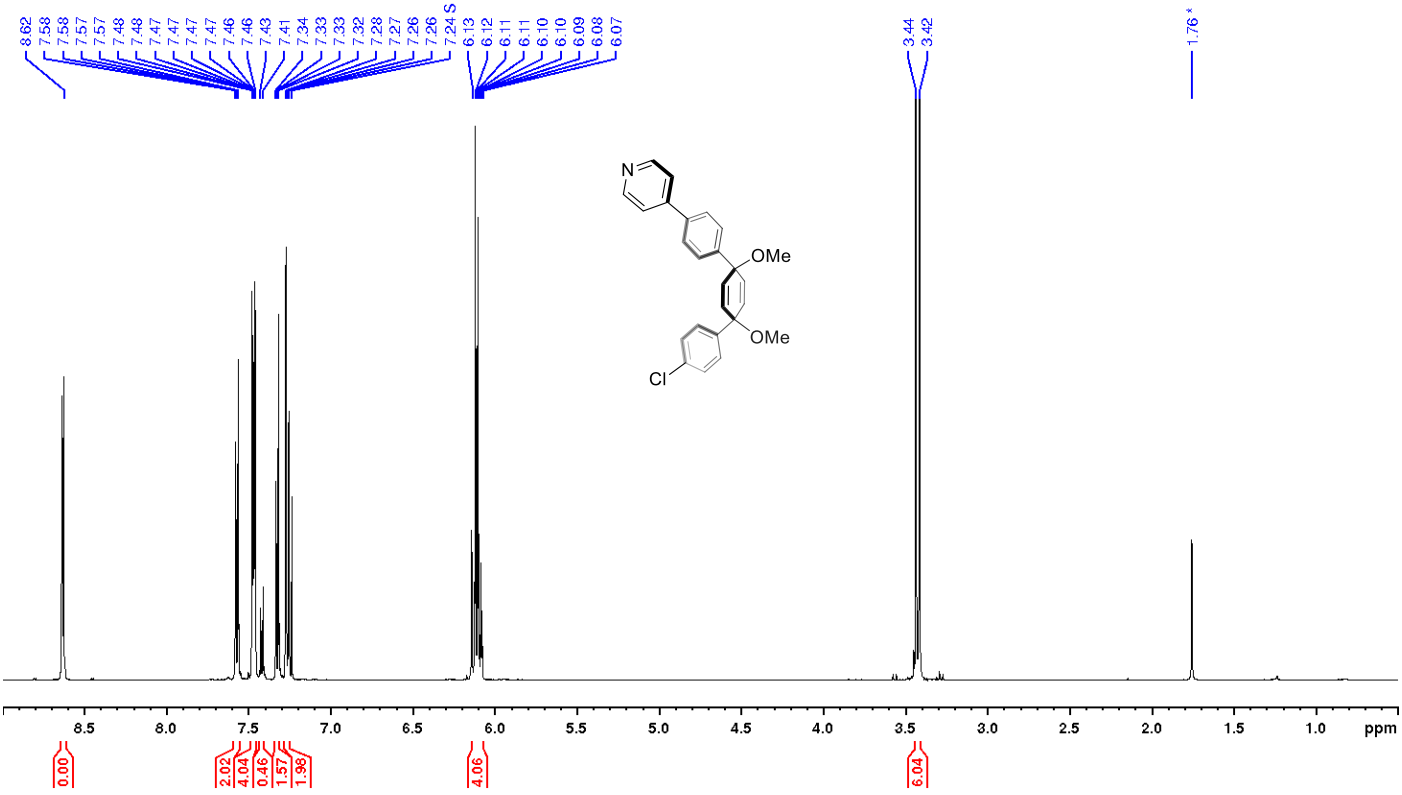

Figure S1. ^{1}H NMR spectrum of **4** (500 MHz, chloroform-*d*, 300 K).

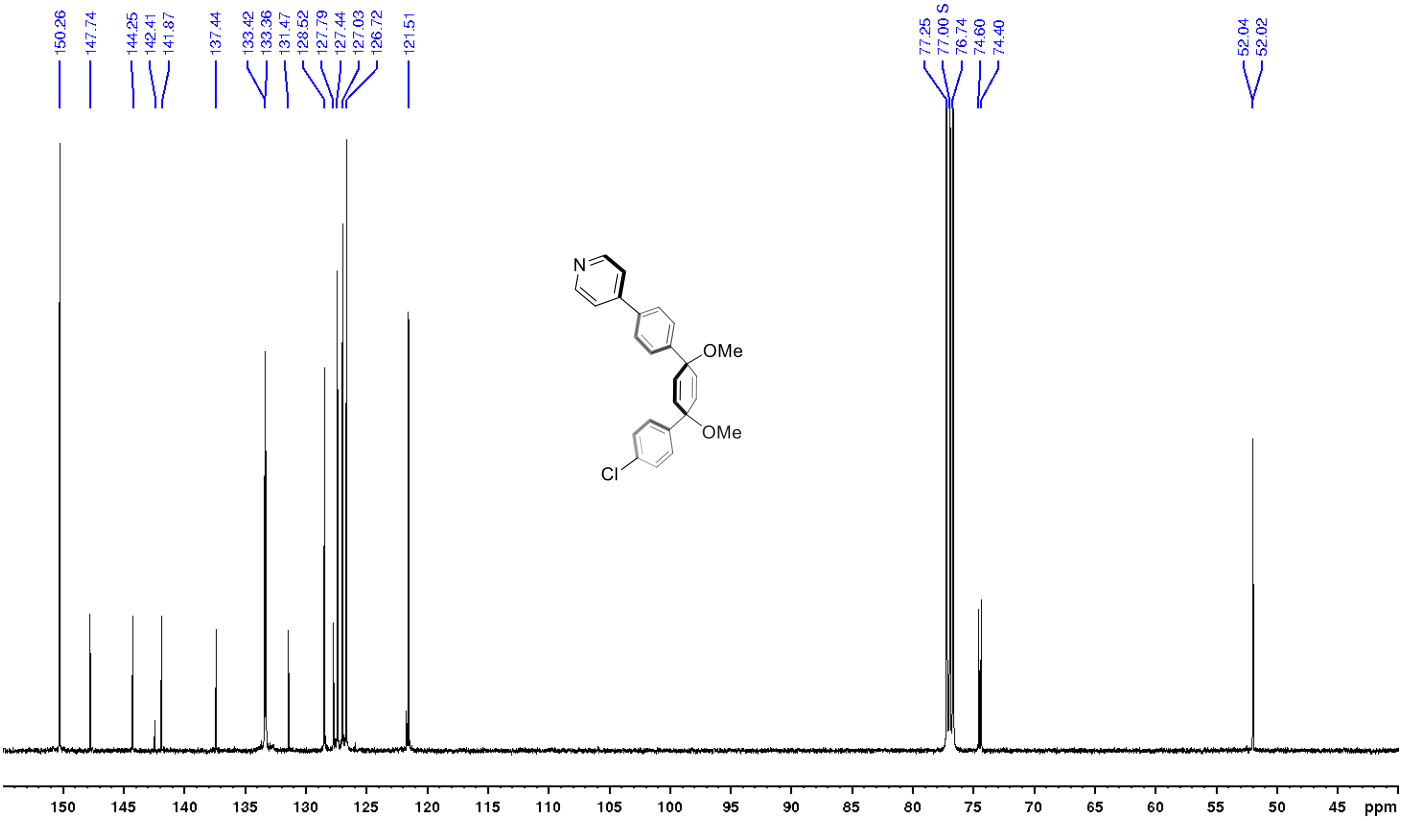

Figure S2. ^{13}C NMR spectrum of **4** (125 MHz, chloroform-*d* , 300 K).

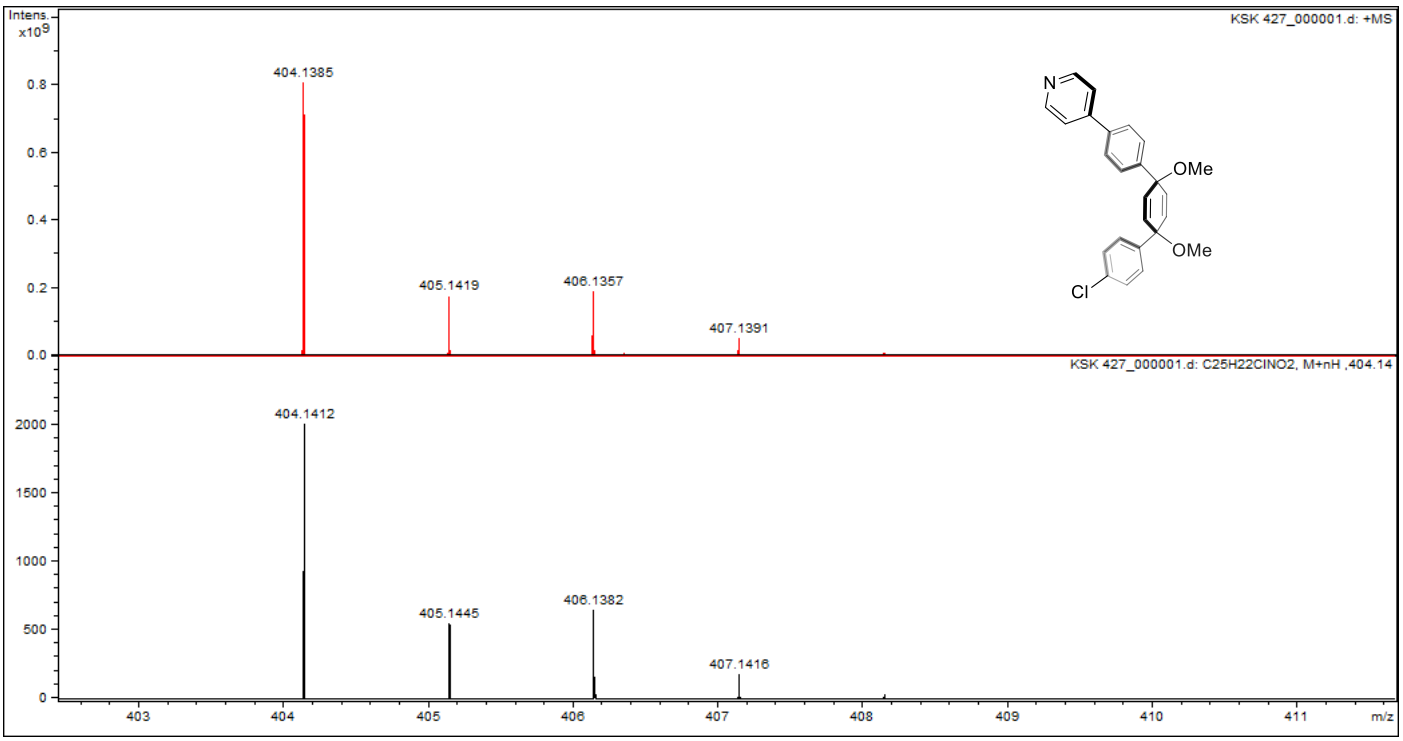

Figure S3. High resolution mass spectrum of **4** (ESI–TOF, top: experimental, bottom: simulated).

4,4'-((1's,4's)-1',1'''',4',4''''-Tetramethoxy-1',1'''',4',4''''-tetrahydro-[1,1':4',1'':4'',1''':4''',1'''':4'''',1''''':4''''',1'''''-sexiphenyl]-4,4'''''-diyl)dipyridine (**5**)

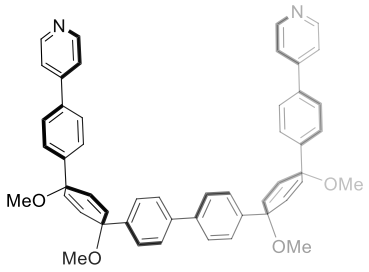

Inside the glove box, $Ni(cod)_2$ (1096 mg, 3.95 mmol, 1.1 equiv), 2,2'-bipyridyl (623 mg, 3.95 mmol, 1.1 equiv), and anhydrous THF (28 mL) were sequentially added to a pressure tube equipped with a stir bar. After 5 min of stirring the above solution, compound **4** dissolved in a mixture of THF (28 mL) and DMF (28 mL) and was added dropwise. The tube was sealed with a Teflon cap, transferred out of glove box, and the mixture was stirred at 85 °C overnight. The reaction mixture was cooled down to room temperature and added to water. The product precipitated and was filtered. The resulting precipitate was redissolved in DCM and purified by using a basic alumina column to afford **5** (90% yield) as a colorless solid.

^{1}H NMR (500 MHz, chloroform-*d*, 300 K): δ 8.61 (4H, d, *J* = 6.1 Hz), 7.51 (12H, m), 6.17 (4H, d, *J* = 10.3 Hz) 6.13 (4H, d, *J* = 10.3 Hz), 3.35 (12H, s).

^{13}C NMR (125 MHz, chloroform-*d*, 300 K): δ 150.30, 147.83, 144.52, 142.50, 140.07, 137.38, 133.69, 133.21, 127.14, 127.03, 126.83, 126.47, 121.55, 74.74, 74.66, 52.08.

HRMS (ESI–TOF): *m/z*: $[M + H]^+$ Calcd for $C_{50}H_{44}N_2O_4$: 737.3374; Found 737.3381.

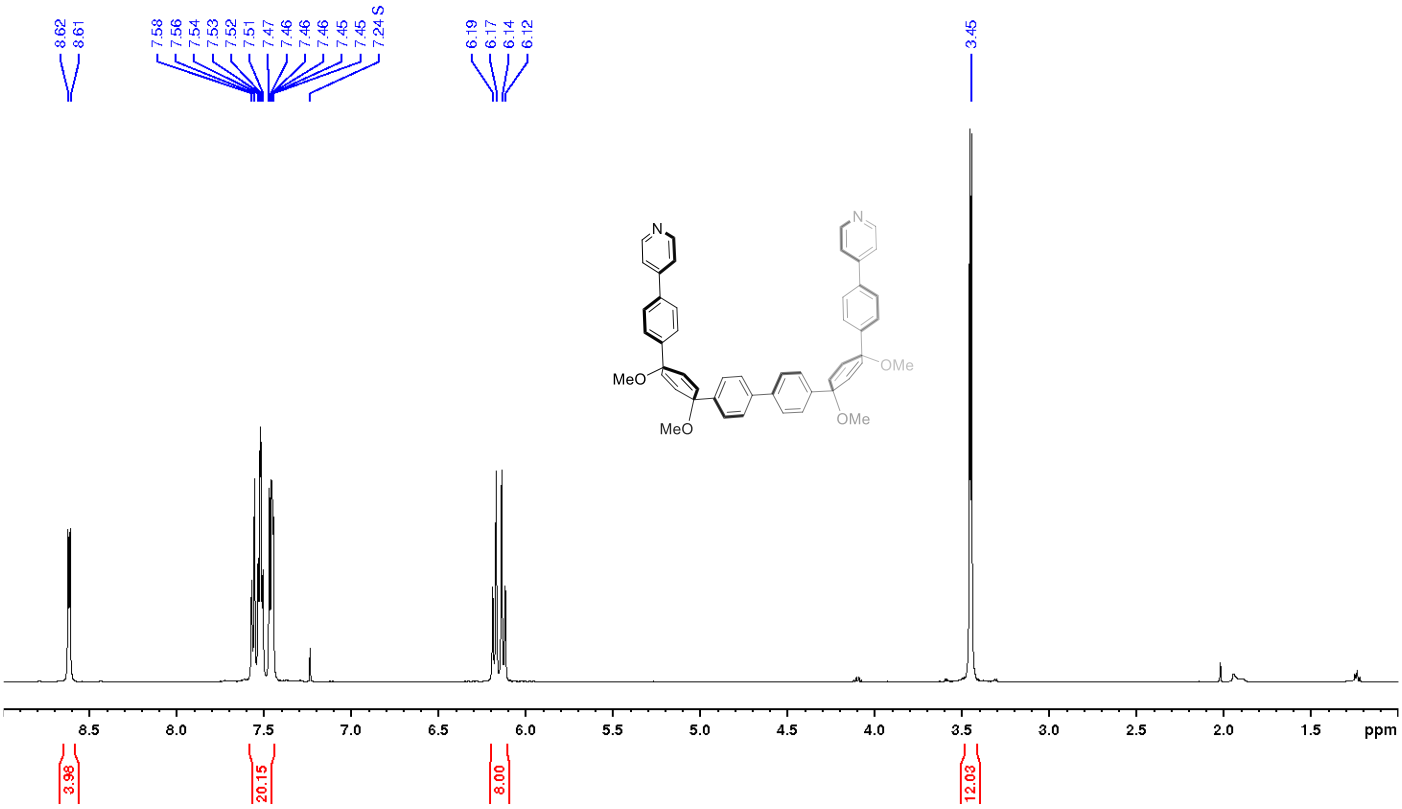

Figure S4. ^{1}H NMR spectrum of **5** (500 MHz, chloroform-*d*, 300 K).

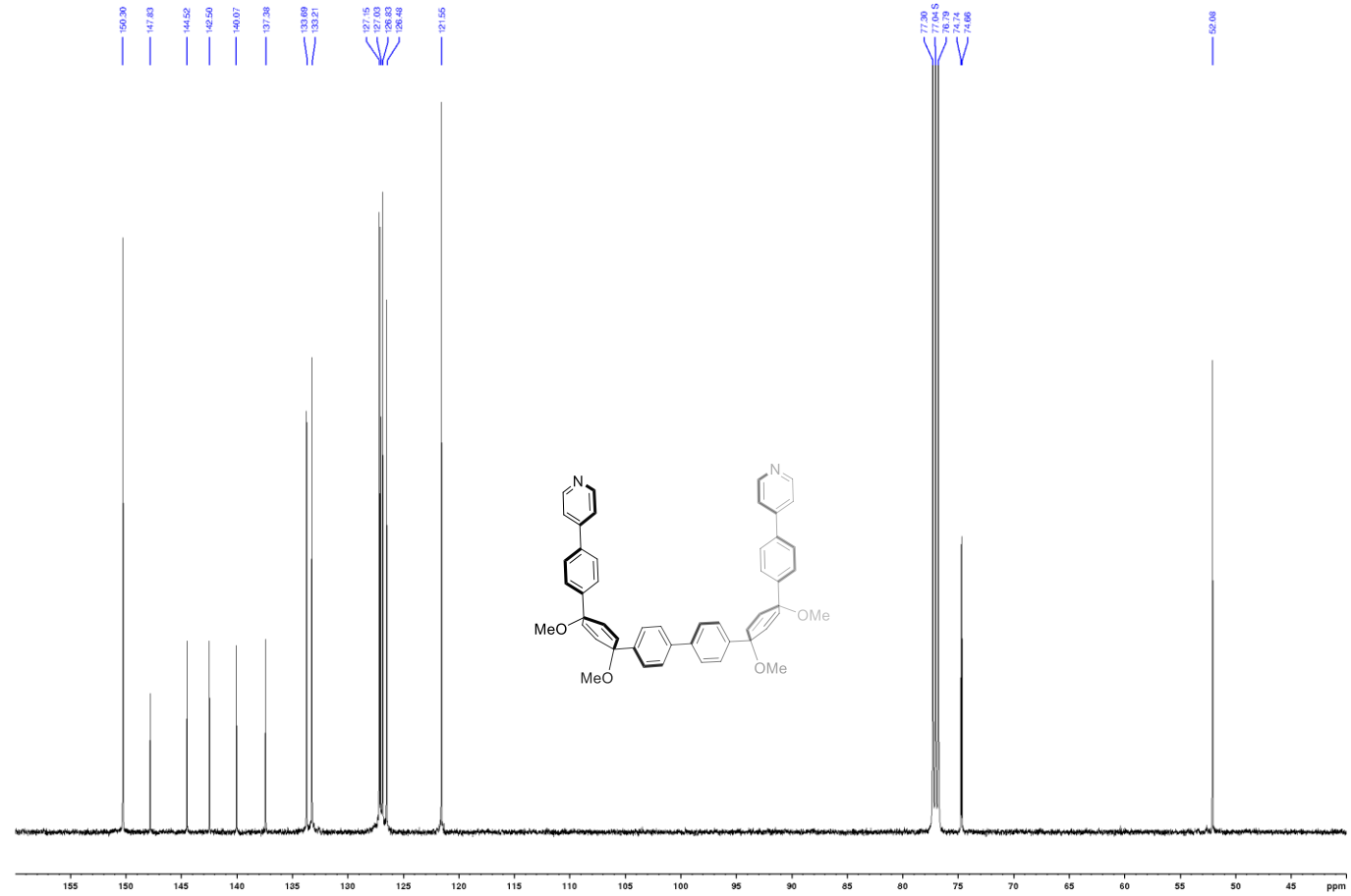

Figure S5. ^{13}C NMR spectrum of **5** (125 MHz, chloroform-*d* , 300 K).

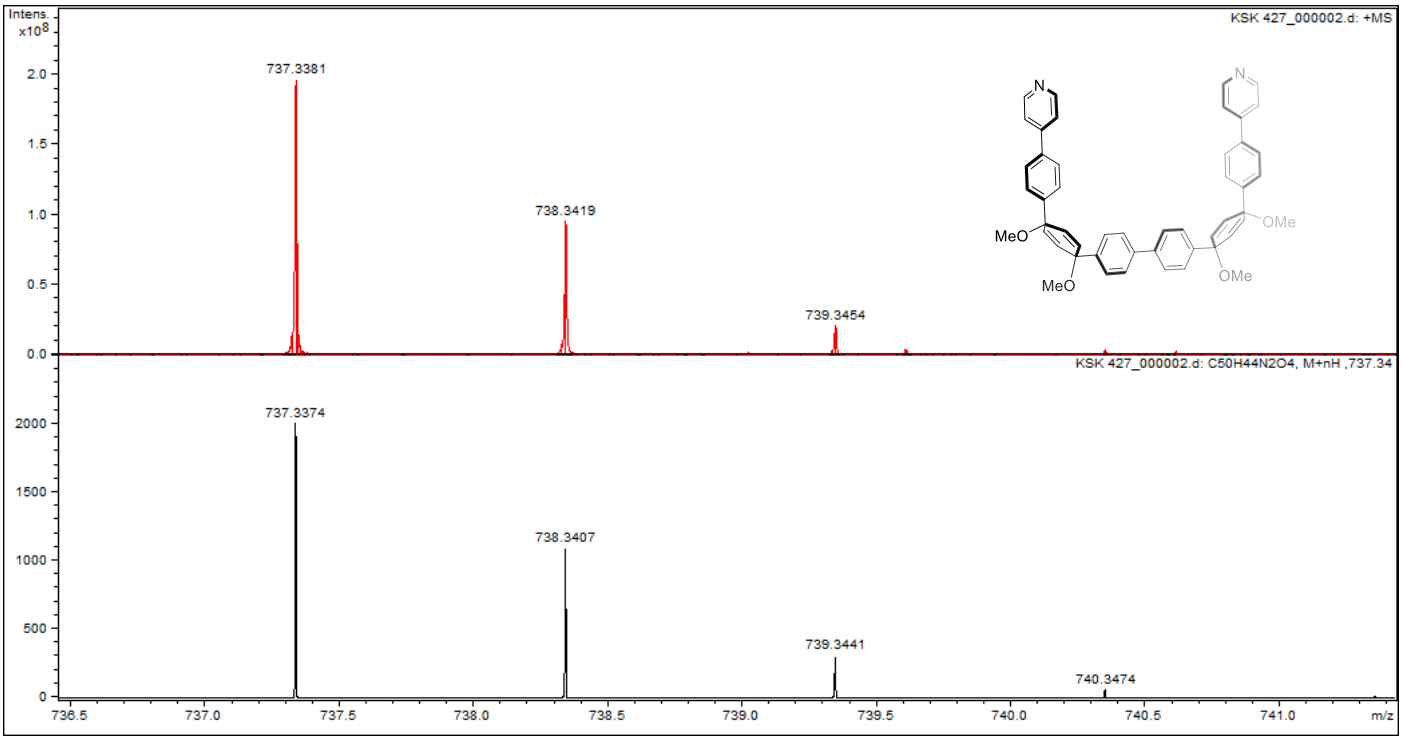

Figure S6. High resolution mass spectrum of **5** (ESI–TOF, top: experimental, bottom: simulated).

Compound [**6**][TFA]$_2$

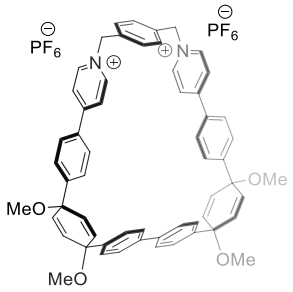

Inside the glove box, α,α'-dibromo-*p*-xylene (81.24 mg, 0.299 mmol, 1.1 equiv), compound **5** (200 mg, 0.271 mmol, 1.0 equiv), and anhydrous DMF (20 mL) were added, to a 35 mL microwave vial equipped with a stir bar. The suspended unclear solution was sealed and transferred from the glove box and stirred at 85 °C for 1.5 h in MW (200 W) power max mode. The clear pale-yellow reaction mixture was cooled down to room temperature and quenched with a saturated aqueous solution of KPF_6. The resulting yellow precipitates were filtered and washed with water several times (98% yield).

^{1}H NMR (500 MHz, DMSO-d_6, 300 K): δ 9.16 (4H, d, *J* = 7.0 Hz), 8.45 (4H, d, *J* = 7.0 Hz), 7.99 (4H, d, *J* = 8.6 Hz), 7.66 (4H, s), 7.60 (4H, d, *J* = 8.6 Hz), 7.54 (4H, d, *J* = 8.5 Hz), 7.36 (4H, d, *J* = 8.5 Hz), 6.19 (4H, d, *J* = 10.4 Hz), 6.15 (4H, d, *J* = 10.4 Hz), 5.8284 (4H, s), 3.38 (6H, s), 3.37 (6H, s).

^{13}C NMR (300 MHz, DMSO-d_6, 300 K): δ 154.8, 147.6, 144.7, 142.6, 138.7, 135.7, 133.9, 1329, 132.6, 129.8, 128.5, 127.0, 126.5, 126.3, 125.1, 99.5, 74.0, 74.0, 62.1, 51.7, 51.6.

HRMS (ESI–TOF): *m/z*: [M + H]$^+$ Calcd for $C_{58}H_{52}N_2OPF_6$: 985.3563; Found 985.3568.

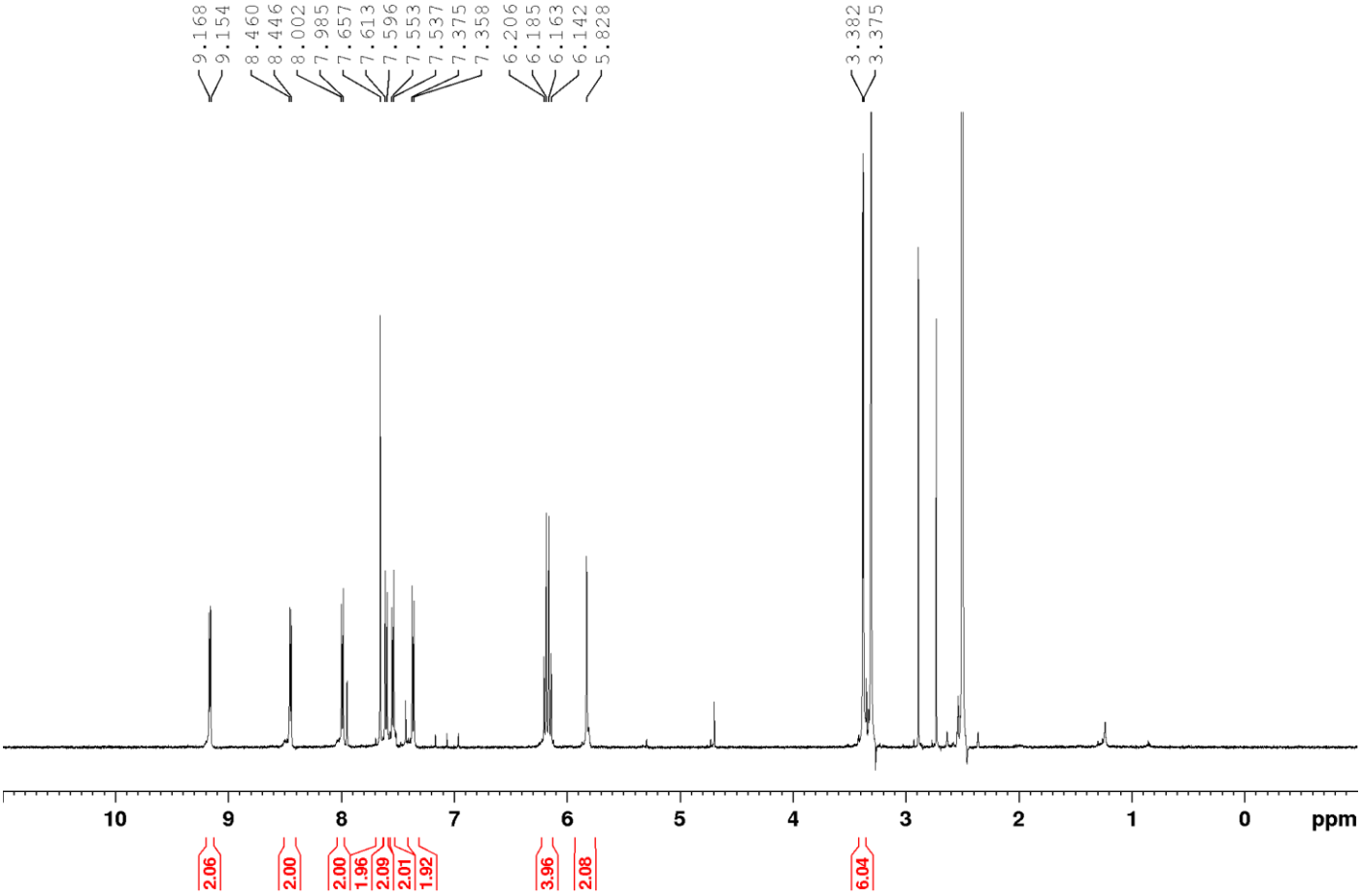

Figure S7. ^{1}H NMR spectrum of 6 (500 MHz, DMSO-d_6, 300 K).

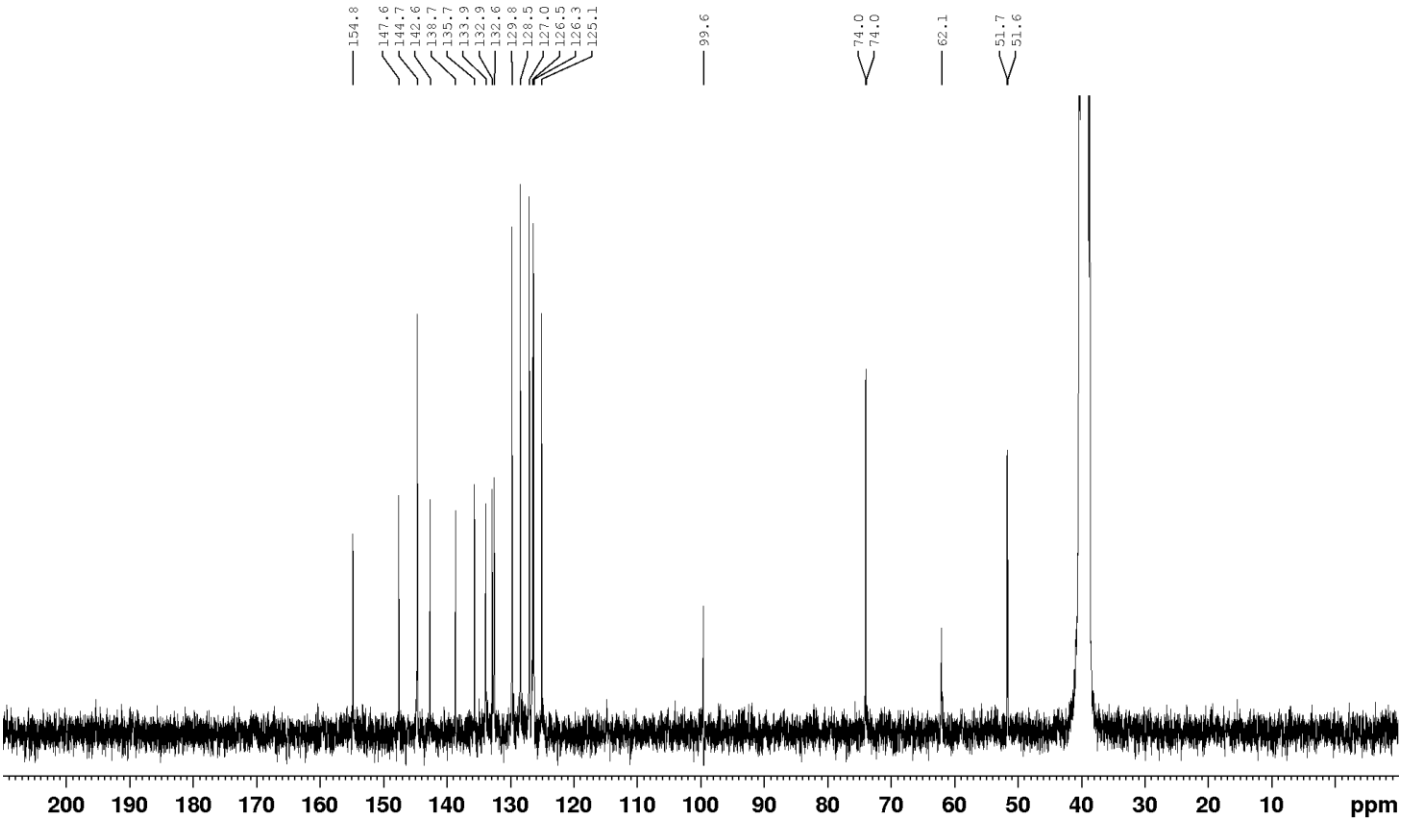

Figure S8. ^{13}C NMR spectrum of 6 (75 MHz, DMSO-d_6, 300 K).

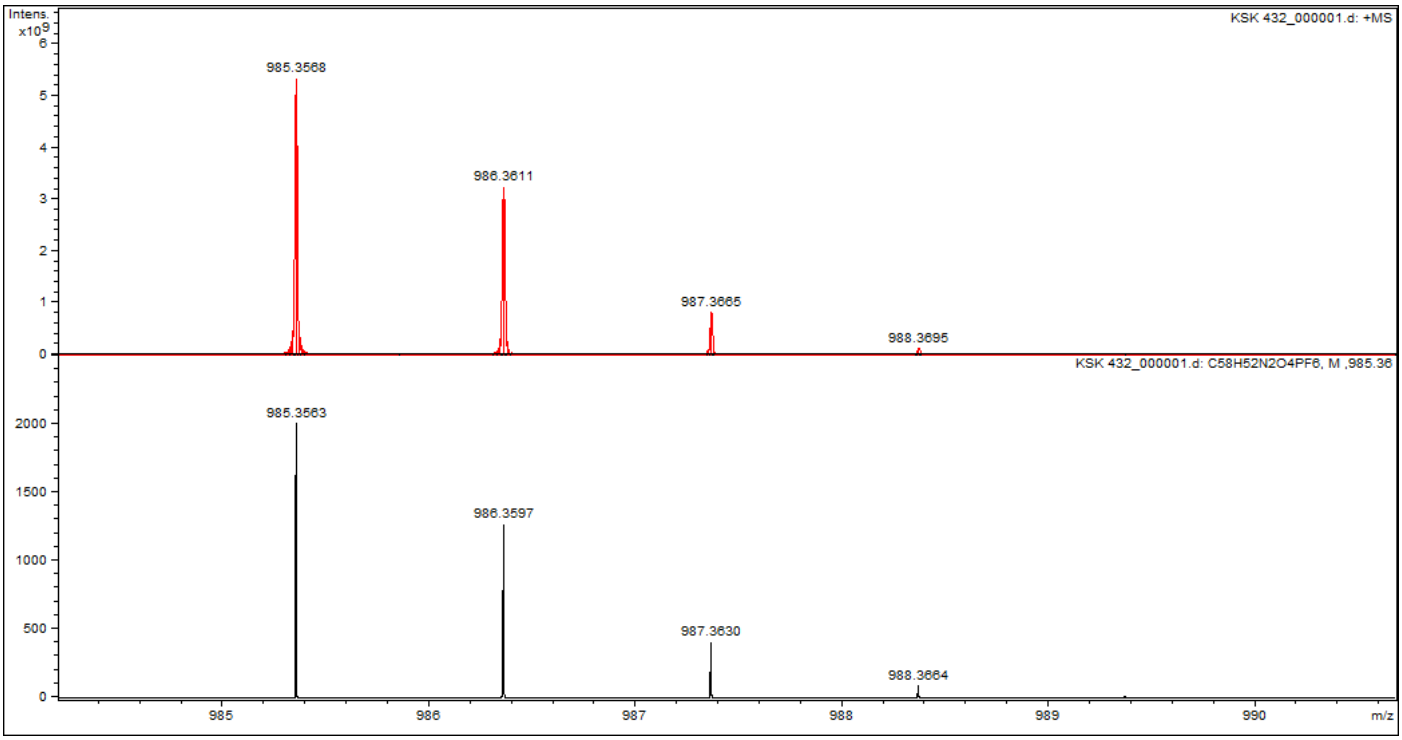

Figure S9. High resolution mass spectrum of **6** (ESI–TOF, top: experimental, bottom: simulated).

Compound [**1**][TFA]$_2$

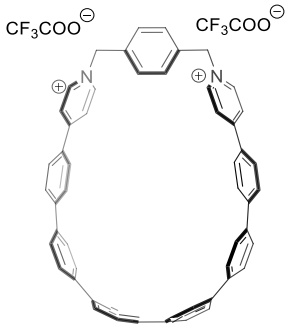

Under a nitrogen atmosphere, concentrated hydrochloric acid (129 µL, 1.89 mmol, 16 equiv) was added to a suspension of $SnCl_2 \cdot 2H_2O$ (220 mg, 0.946 mmol, 8 equiv) in 5.5 mL THF and stirred for 15 min. Subsequently, the resulting mixture was added dropwise to a suspension containing compound **6** (134 mg, 0.118 mmol, 1 equiv) in 9 mL of THF, which immediately turned the pale yellow color to a deep yellow-orange and was vigorously stirred at RT for 4 h. To the resulting mixture, a saturated aqueous KPF_6 solution was added. After 2 h precipitate was filtered off, washed three times with water, and dried. The product was extracted from the solid with a few portions of 1% solution of TFA in mehanol. Combined filtrates were concentrated under reduced pressure. The product was precipitated by adding water, filtered off, and dried. The final purification was made by GPC chromatography, followed by concentration under reduced pressure, precipitation from the water, filtration, and drying under vacuum (12% yield).

^{1}H NMR (500 MHz, acetonitrile-d_3, 300 K): δ 8.68 (4H, d, J = 6.9 Hz), 8.20 (4H, d, J = 6.7 Hz), 7.91 (4H, d, J = 8.9 Hz), 7.80 (4H, d, J = 9.2 Hz), 7.73-7.69 (16H, m), 7.42 (4H, s), 5.69 (4H, s).

^{13}C NMR (125 MHz, acetonitrile-d_3, 300 K): δ 156.34, 145.06, 144.51, 140.23, 138.73, 137.70, 136.87, 135.82, 131.91, 130.04, 129.43, 128.41, 128.39, 128.33, 128.27, 128.19, 125.27, 63.37.

HRMS (ESI–TOF): m/z: $[M + H]^+$ Calcd for $C_{54}H_{40}N_2PF_6$: 861.2828; Found 861.2854.

UV-vis (DMF, 300 K) λ [nm] (ε in M^{-1} cm^{-1}): 288 (32360), 345 (52863).

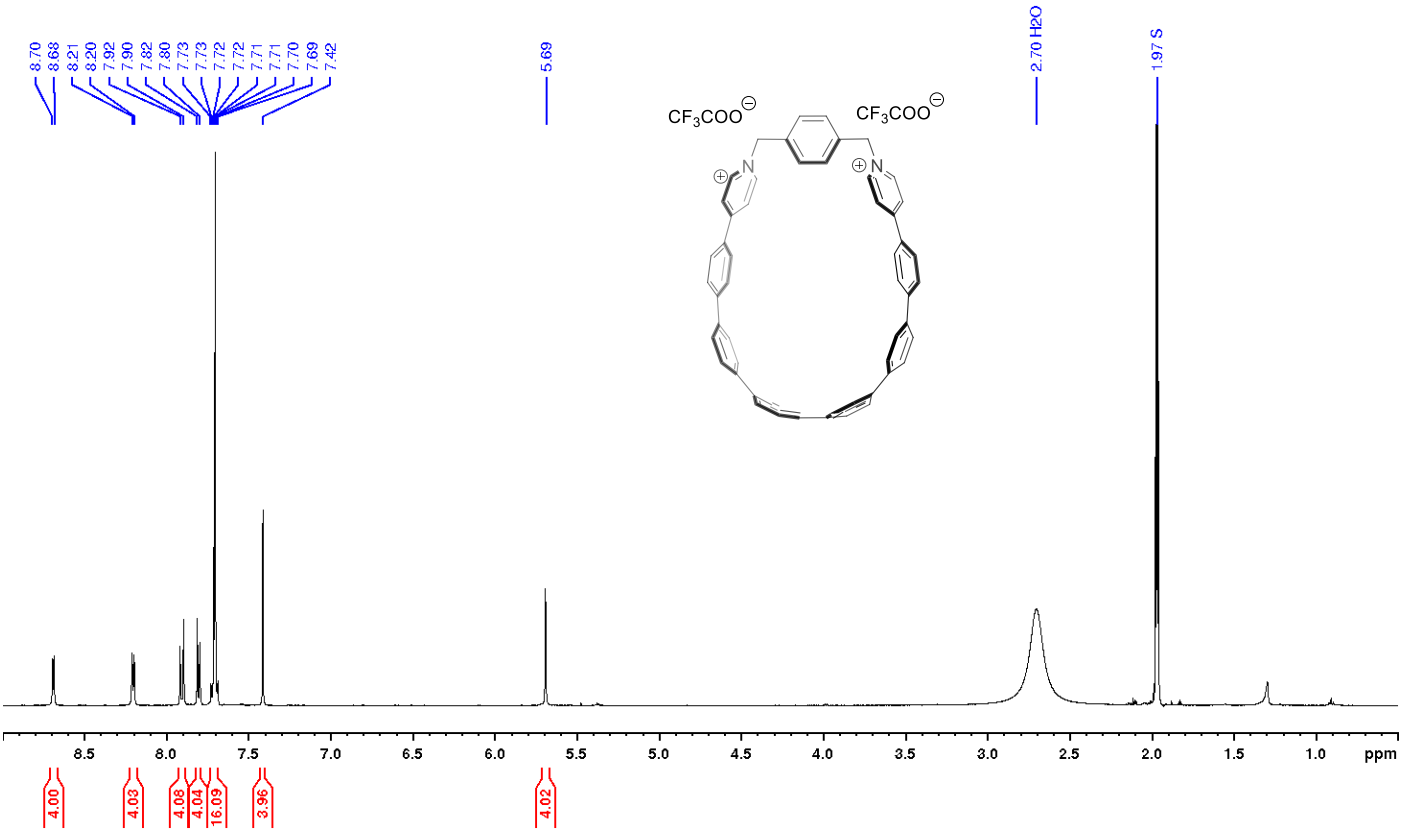

Figure S10. ^{1}H NMR spectrum of [**1**][TFA]$_2$ (500 MHz, acetonitrile-d_3, 300 K).

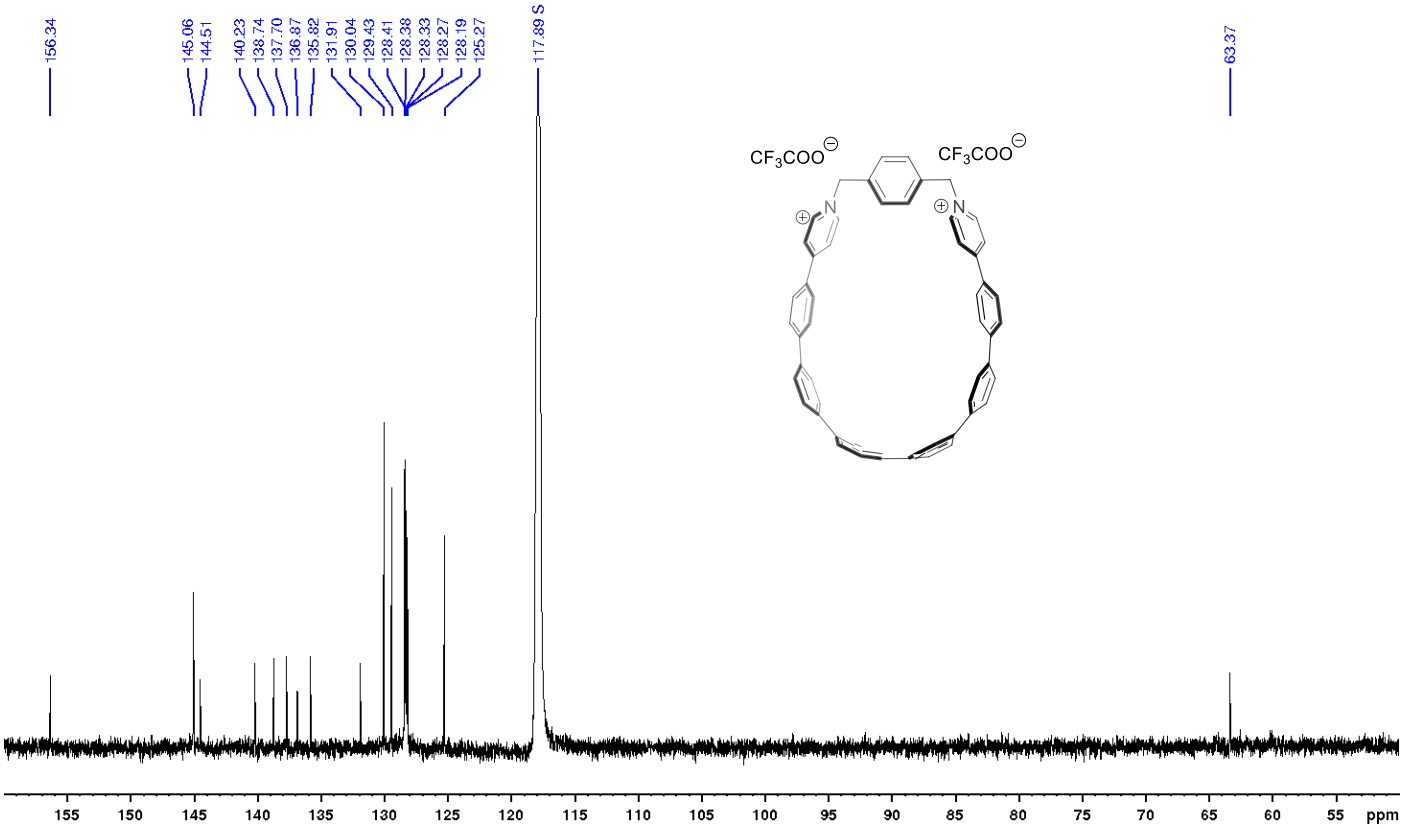

Figure S11. ^{13}C NMR spectrum of [**1**][TFA]$_2$ (125 MHz, acetonitrile-d_3, 300 K).

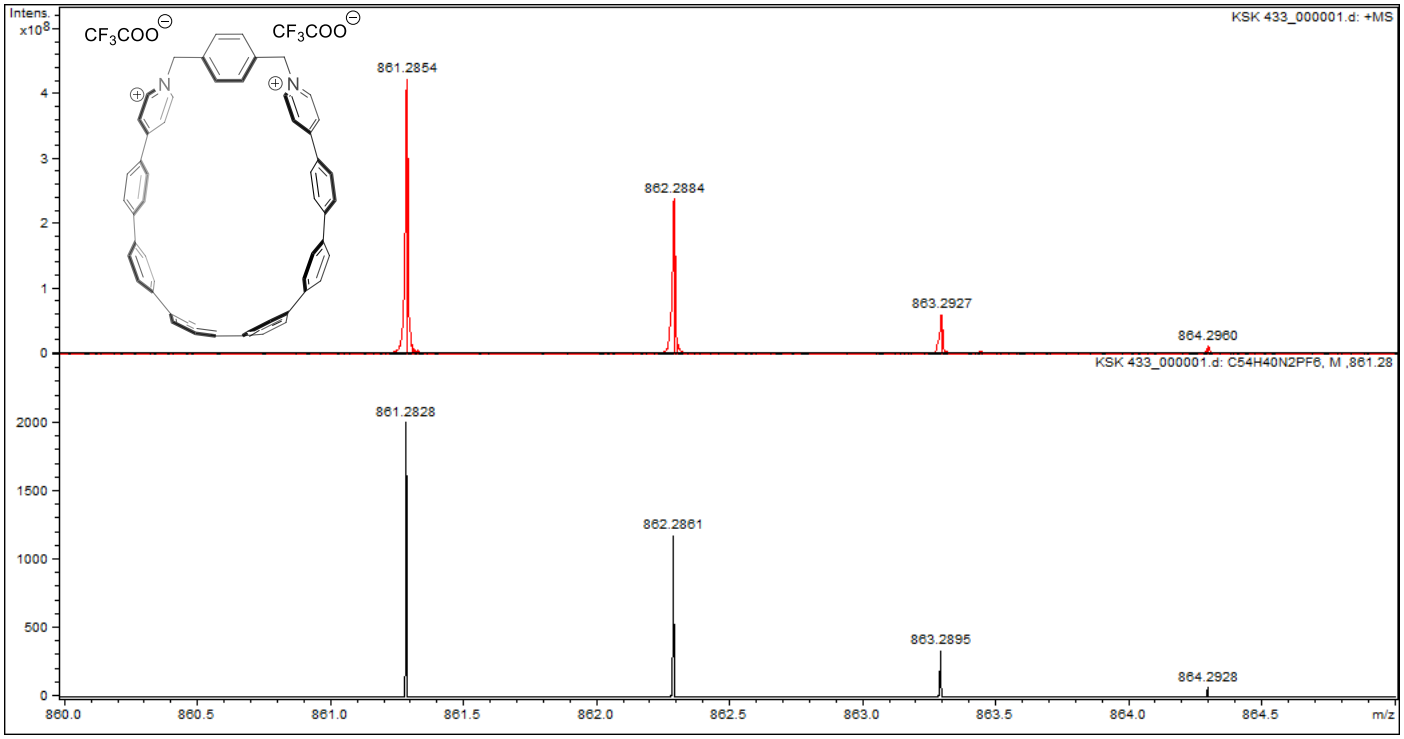

Figure S12. High resolution mass spectrum of [**1**][TFA]$_2$ (ESI–TOF, top: experimental, bottom: simulated).

Compound [**2**][TFA]$_2$

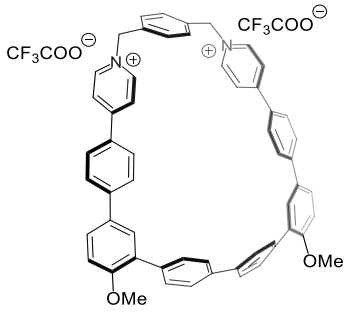

Under a nitrogen atmosphere, concentrated sulfuric acid (4.79 mL, 88.1 mmol, 160 equiv) was added dropwise to a vigorously stirring solution of compound **6** in 78 mL of MeOH. After 2 h of stirring in RT, the saturated aqueous solution of KPF_6 was added. The formed precipitate was filtrated, washed 3 times with water and dried under the vacuum. Pure compound [**2**][TFA]$_2$ was obtained after 2 cycles of purification on RF HPLC in 1% TFA in acetonirile.

^{1}H NMR (600 MHz, acetonitrile-d_3, 300 K): δ 8.71 (4H, d, J = 7.1 Hz), 8.19 (4H, d, J = 7.1 Hz), 7.85 (4H, d, J = 8.6 Hz) 7.68 (10H, m), 7.52 (4H, s), 7.50 (4H, d, J = 8.4 Hz), 7.21 (2H, d, J = 8.5 Hz), 6.83(2H, d, J = 2.5 Hz), 5.70 (4H, s), 3.96 (6H, s).

^{13}C NMR (151 MHz, acetonitrile-d_3, 300 K): δ 157.6, 157.5, 146.2, 145.2, 140.7, 139.8, 136.1, 136.0, 133.2, 132.7, 132.2, 131.0, 130.8, 129.6, 129.3, 127.8, 127.1, 125.9, 113.0, 63.9, 56.6.

HRMS (ESI–TOF): m/z: $[M]^{2+}$ Calcd for $C_{56}H_{44}N_2O_2$: 388.1696; Found 388.1697.

UV-vis (DMF, 300 K) λ [nm] (ε in M^{-1} cm^{-1}): 280 (27558), 313.5 (27904), 356.5 (26884).

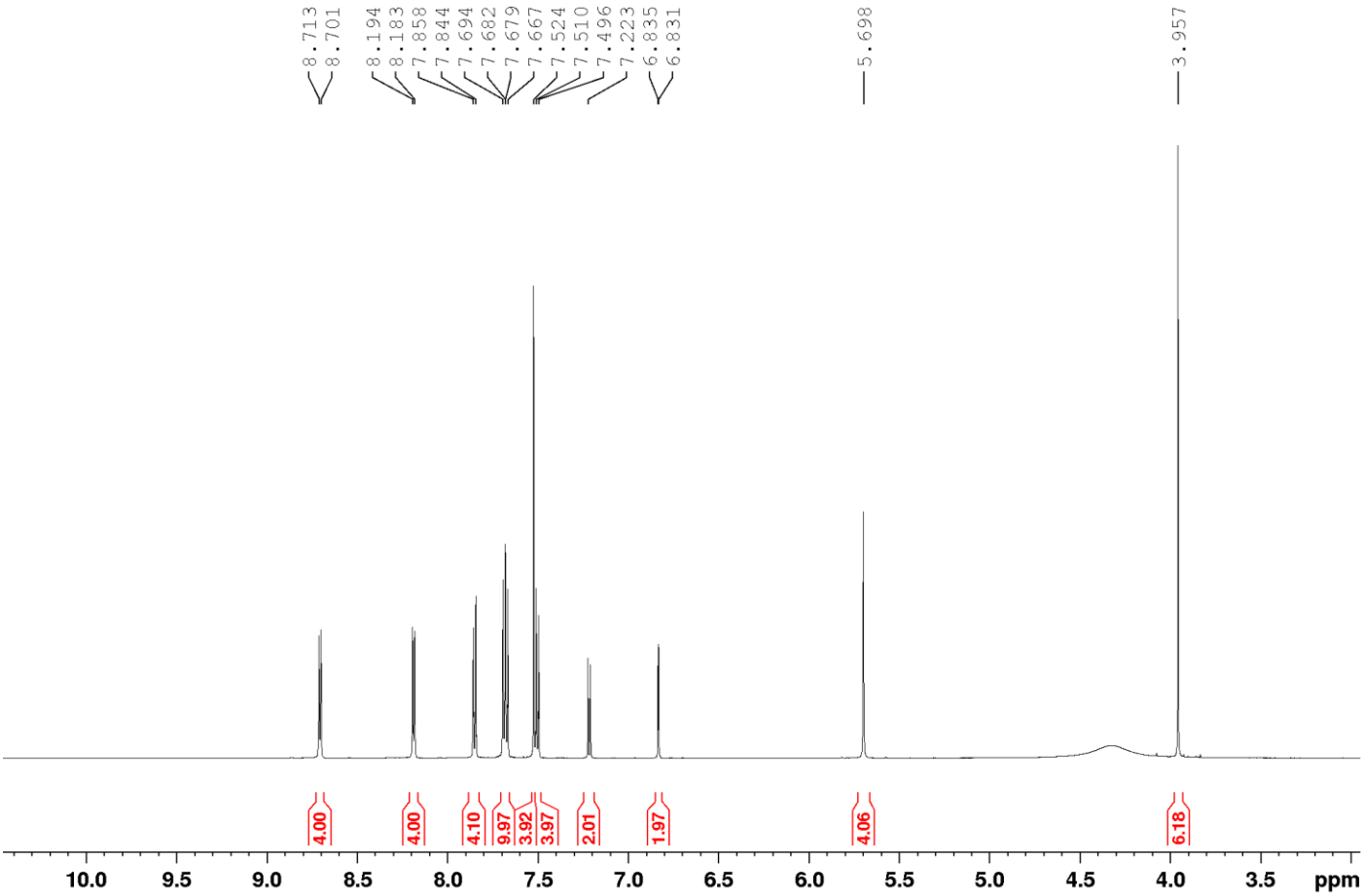

Figure S13. ^{1}H NMR spectrum of [**2**][TFA]$_2$ (600 MHz, acetonitrile-d_3, 300 K).

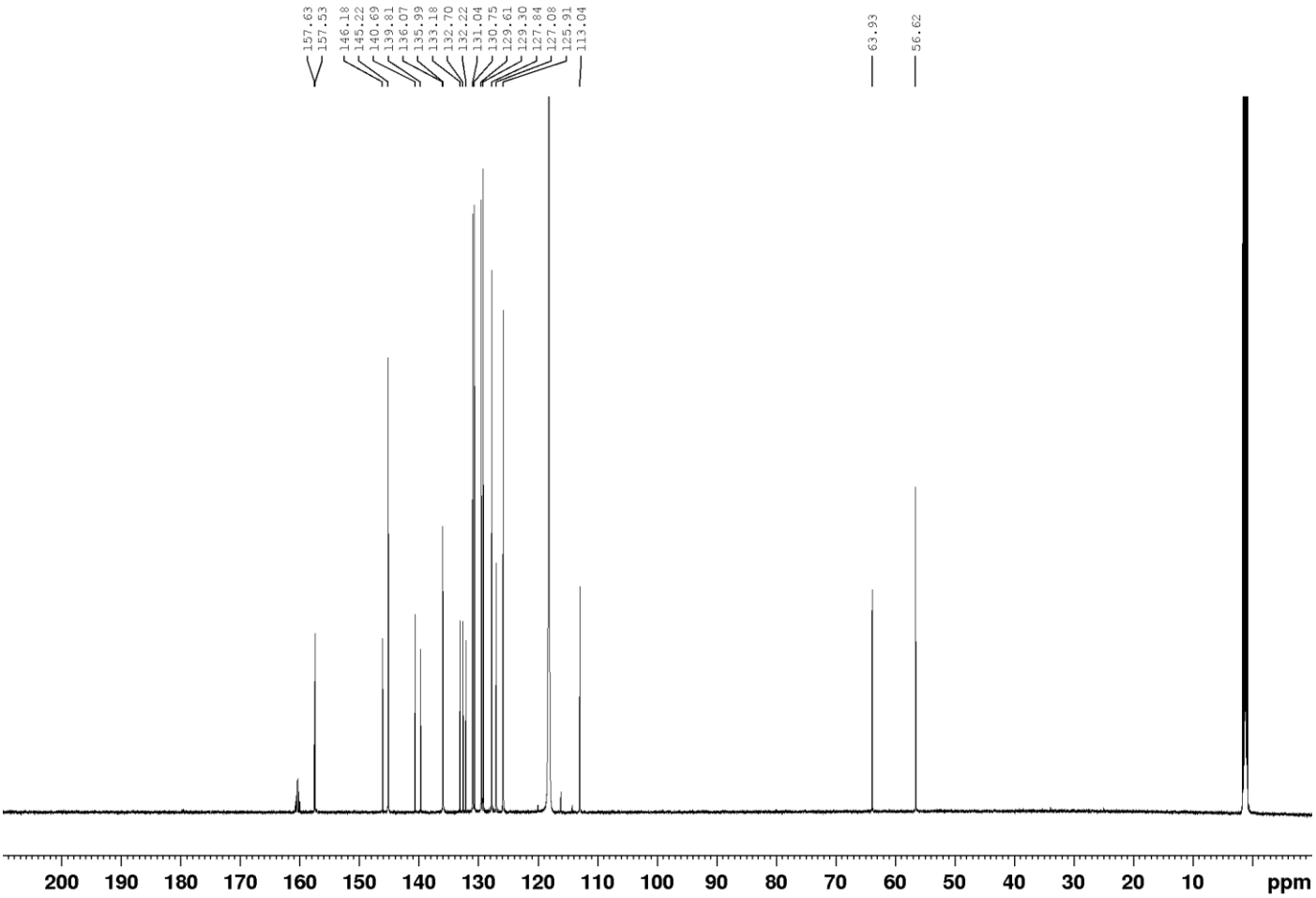

Figure S14. ^{13}C NMR spectrum of [**2**][TFA]$_2$ (151 MHz, acetonitrile-d_3, 300 K).

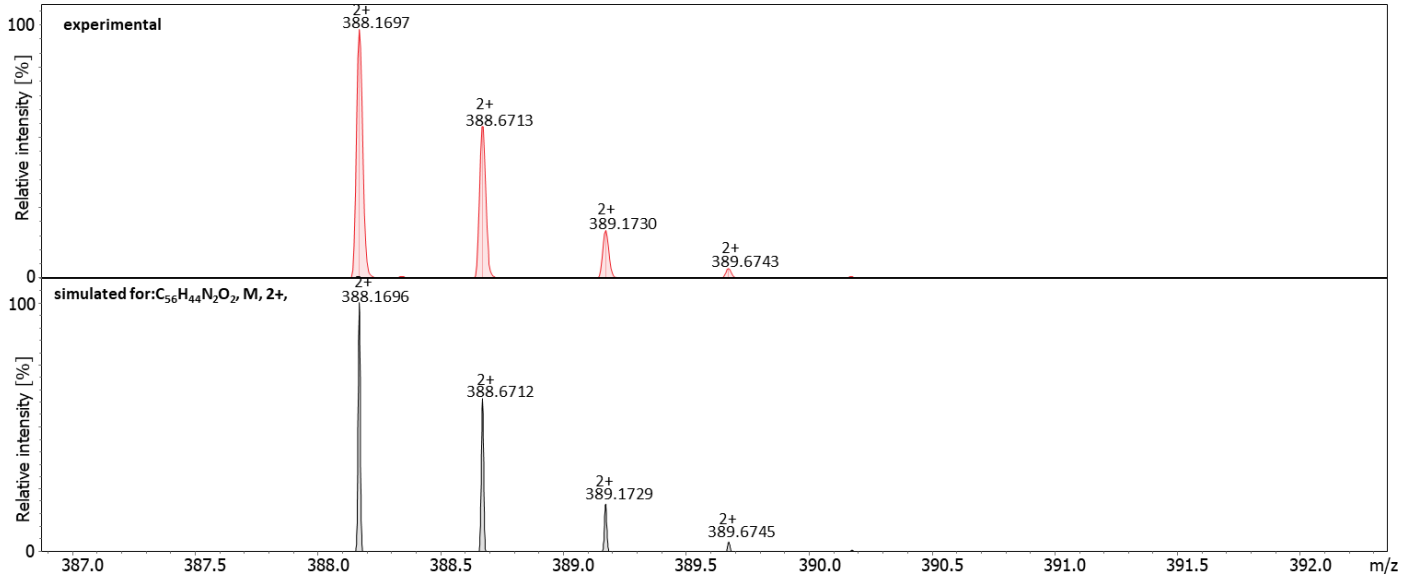

Figure S15. High resolution mass spectrum of [**2**][TFA]$_2$ (ESI–TOF, top: experimental, bottom: simulated).

3. Additional Schemes

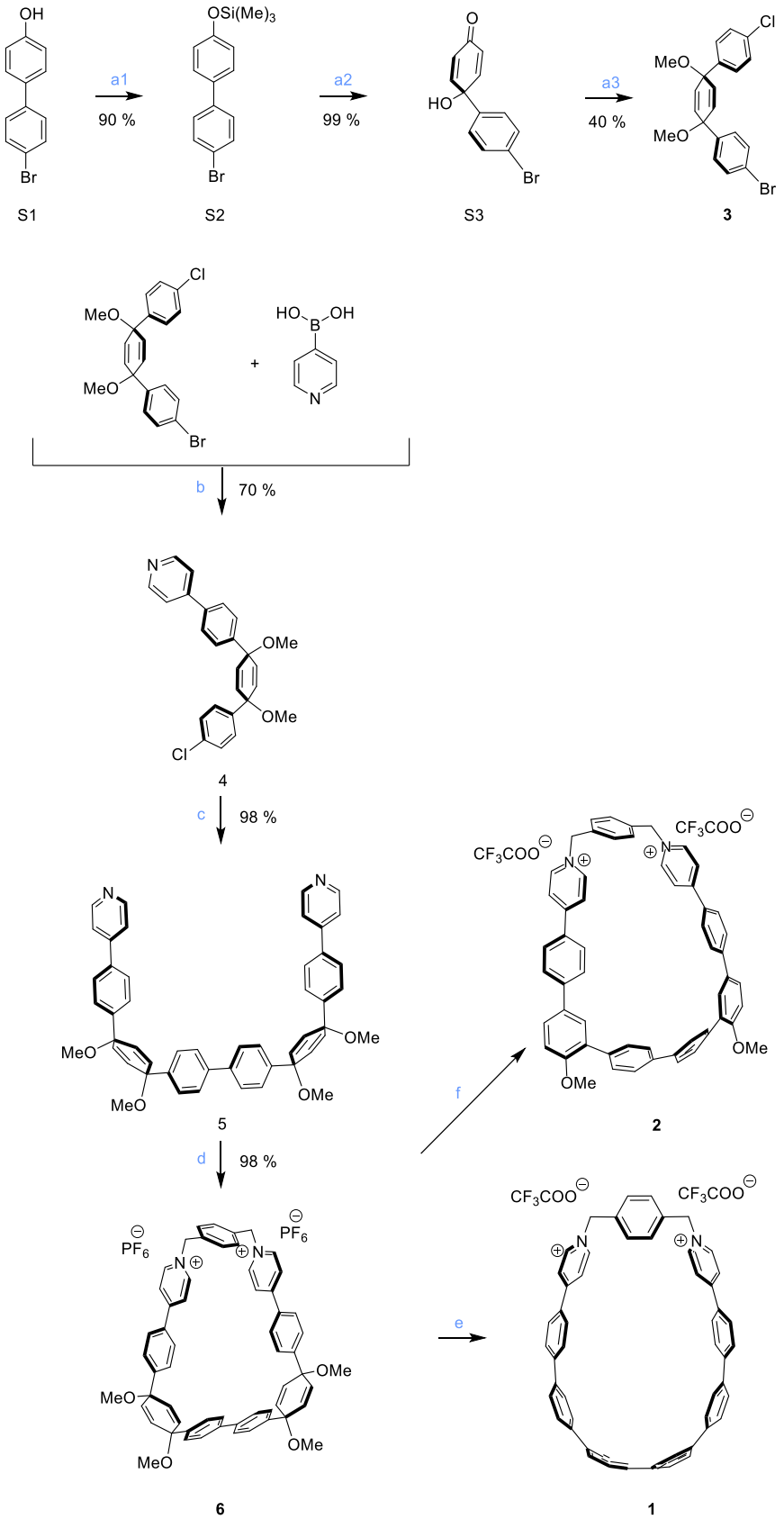

Scheme S1. Synthesis of [**1**][TFA]$_2$ and [**2**][TFA]$_2$. Reagents and conditions: (b) Pd(PPh$_3$)$_4$, K$_2$CO$_3$, 1,4-dioxane, MW, 100 °C, 2 h; (c) Ni(COD)$_2$, bpy, THF, DMF, 85 °C, ovn; (d) 1) DMF, MW, 85 °C, 1.5 h; 2) H$_2$O, KPF$_6$; (e) 1) H$_2$SnCl$_4$, THF, 4 h; 2) H$_2$O, KPF$_6$; 3) 1% TFA in MeOH, 4) GPC; (f) 1) H$_2$SO$_4$, MeOH, 2 h; 2) H$_2$O, KPF$_6$; 3) reverse-phase HPLC in 1% TFA in acetonitrile.

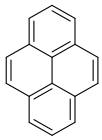

P

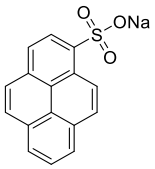

[**PMS**]Na

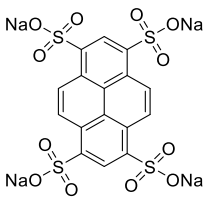

[**TSP**]Na_4

Scheme S2. Structures of the guests molecules.

4. Experimental Data

4.1. Chromatography

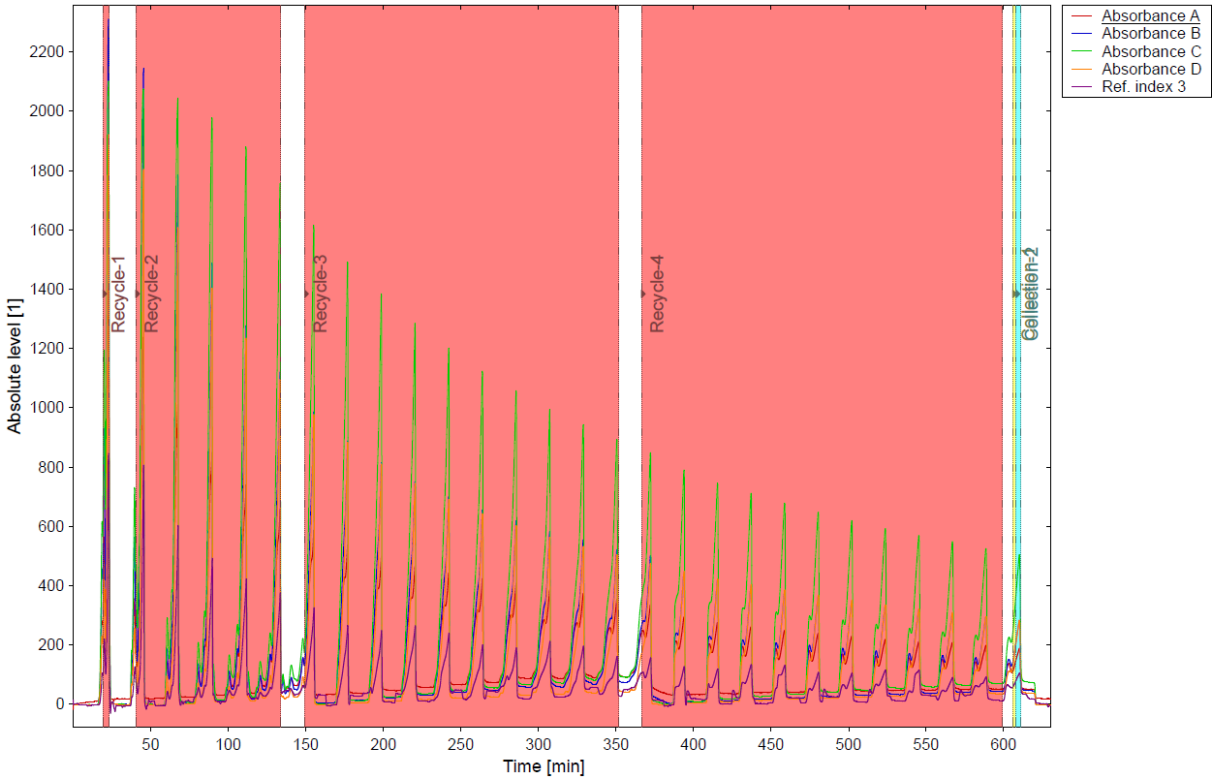

Figure S16. GPC chromatogram for compound [**1**][TFA]$_2$ purification. Wavelenghts: A = 254 nm, B = 310 nm, C = 350 nm, D = 415 nm.

4.2. NMR Spectroscopy

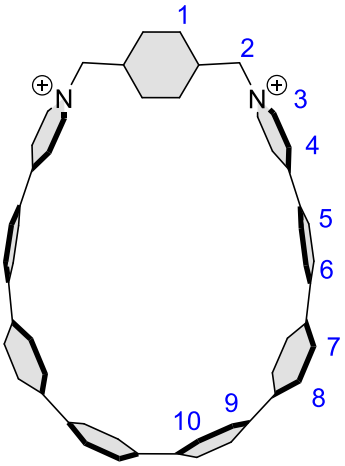

$[\mathbf{1}]^{2+}$

^{1}H NMR [ppm]:
1. 7.42
2. 5.69
3. 8.68
4. 8.20
5. 7.91
6. 7.80
7-10. 7.73-7.69

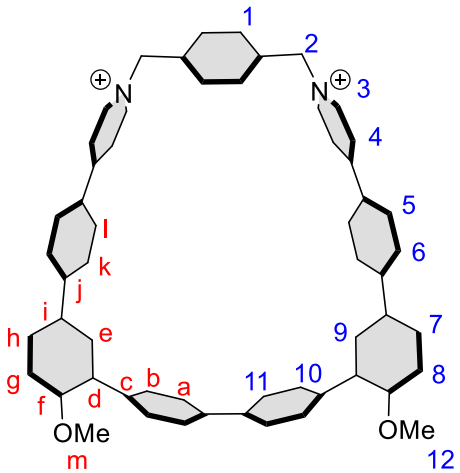

$[\mathbf{2}]^{2+}$

^{1}H NMR [ppm]:
1. 7.52
2. 5.70
3. 8.71
4. 8.19
5. 7.85
6,7,10. 7.68
8. 7.21
9. 6.83
11. 7.50
12. 3.96

^{13}C NMR [ppm]:
a. 130.8
b. 127.8
c. 140.7
d. 139.8
e. 136.0
f. 157.5
g. 113.0
h. 127.1
i. 146.2
j. 146.2
k. 129.3
l. 129.6
m. 56.6

Scheme S3. ^{1}H and ^{13}C NMR chemical shifts of [**1**][TFA]$_2$ and [**2**][TFA]$_2$. The assignment was based on data obtained from COSY, NOESY, HSQC and HMBC experiments.

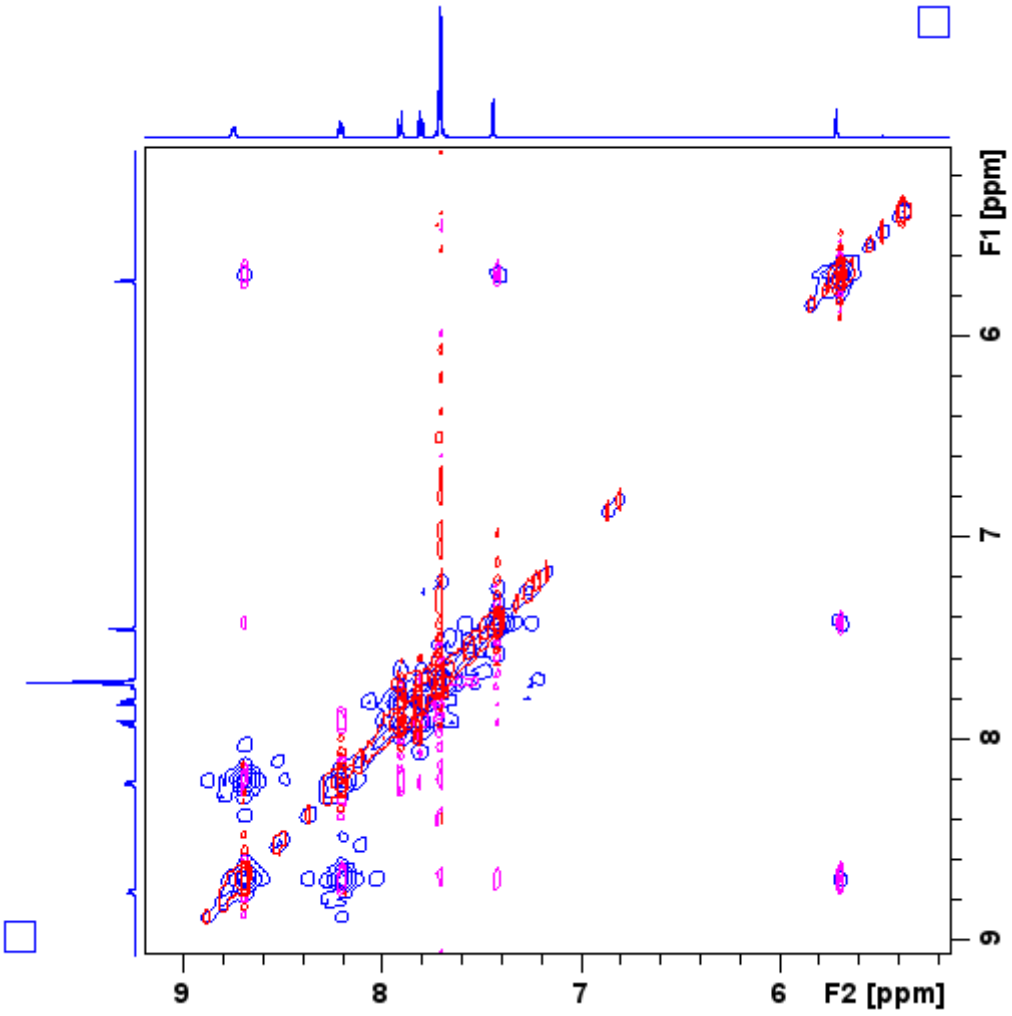

Figure S17. Overlayed COSY (blue) and NOESY (red/pink) spectra of [**1**][TFA]$_2$ (500 MHz, CD_3CN, 300 K) .

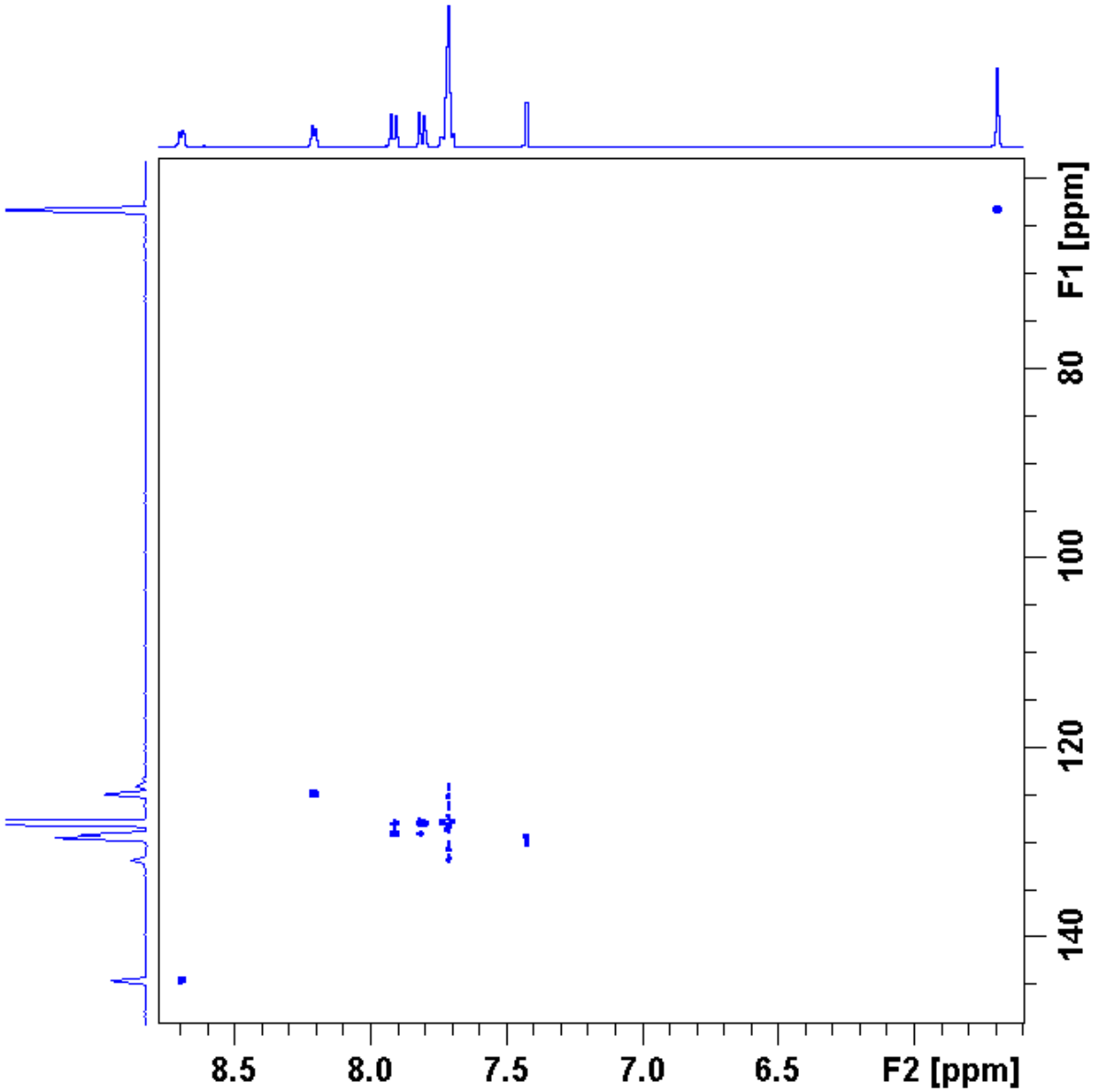

Figure S18. HSQC spectrum of [**1**][TFA]$_2$ (500 MHz, CD_3CN, 300 K).

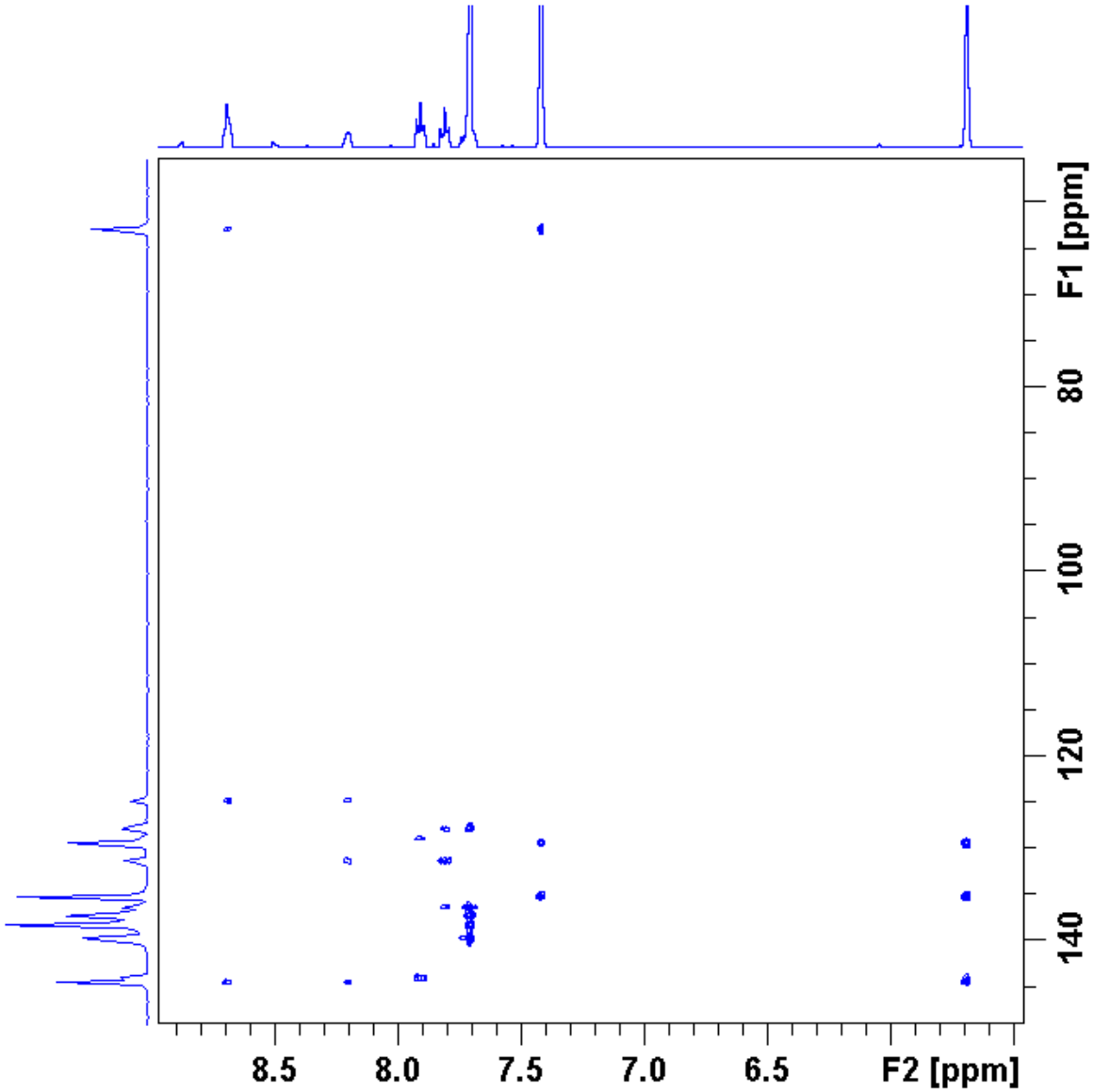

Figure S19. HMBC spectrum of [**1**][TFA]$_2$ (500 MHz, CD_3CN, 300 K).

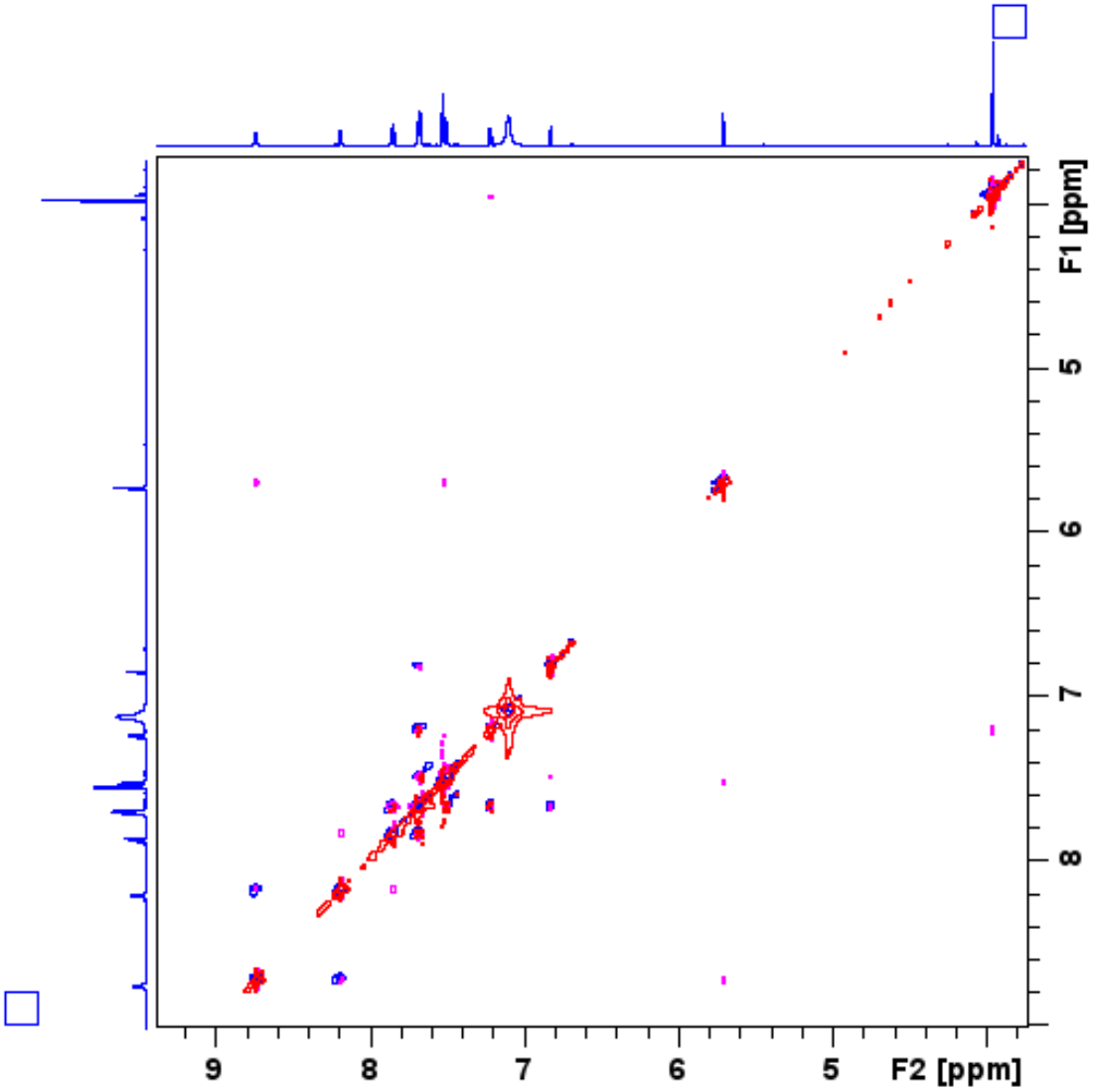

Figure S20. Overlayed COSY (blue) and NOESY (red/pink) spectra of [**2**][TFA]$_2$ (600 MHz, CD_3CN, 300 K) .

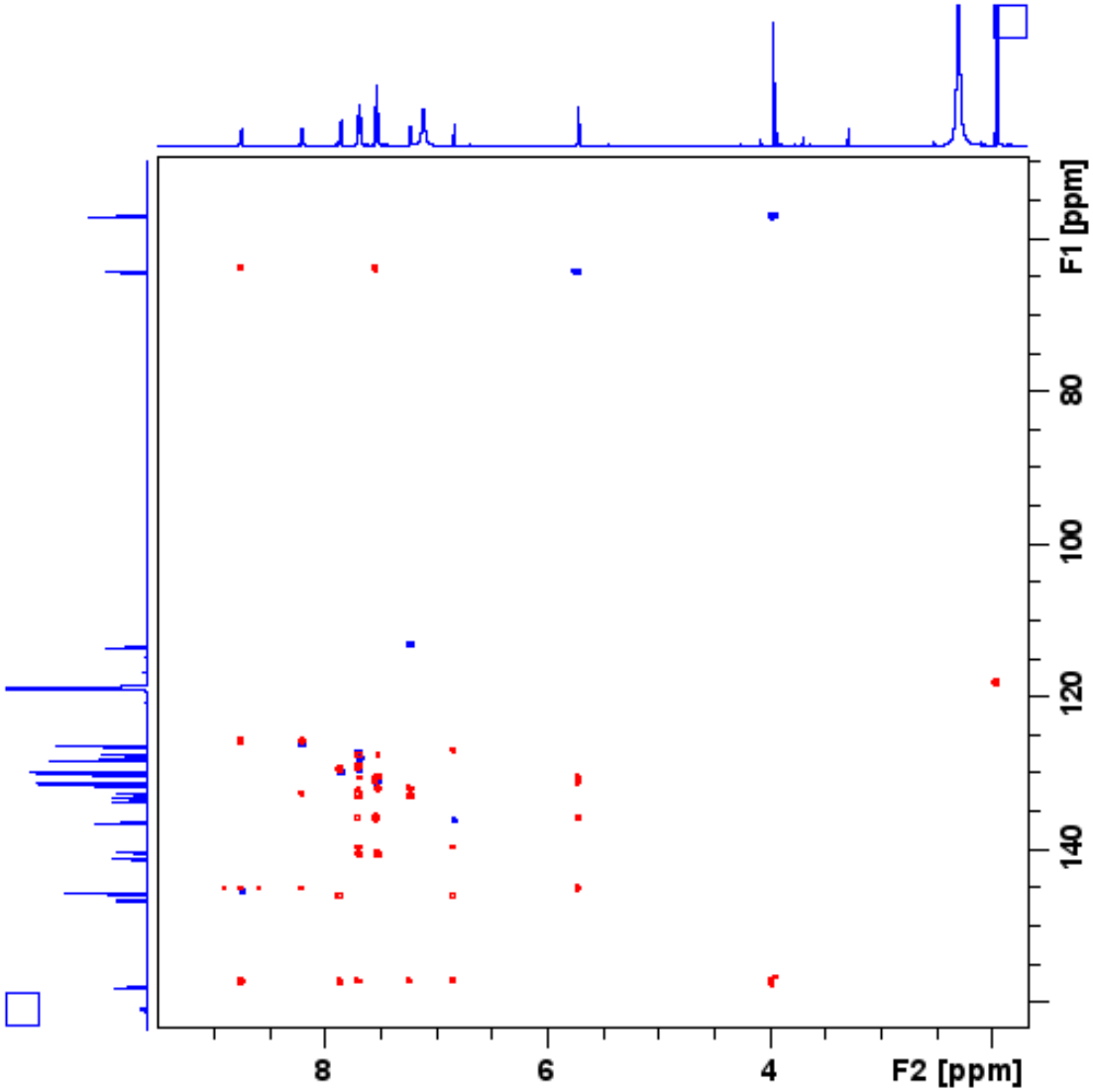

Figure S21. Overlayed HSQC (blue/green) and HMBC (red) spectra of [**2**][TFA]$_2$ (600 MHz, CD_3CN, 300 K).

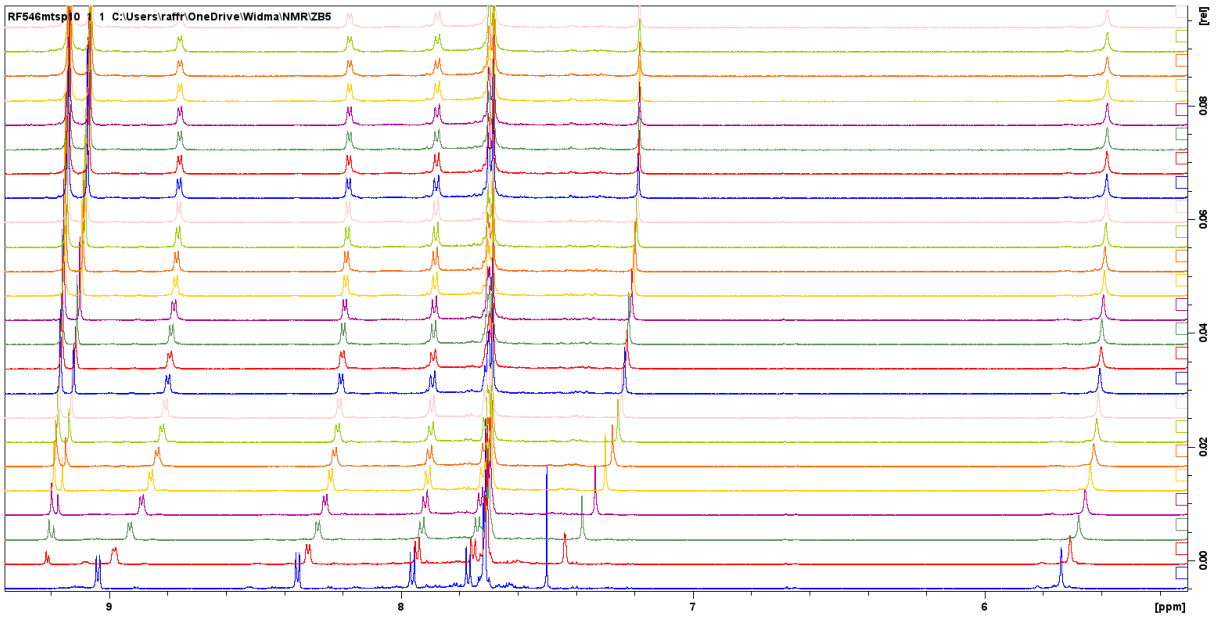

Figure S22. ^{1}H NMR titration spectra (600 MHz, 10% D_2O in DMSO-d_6, 300 K) obtained upon addition of 0–6.92 equiv. of a 9.00 mM solution of $[Na]_4[TSP^{4-}]\cdot 7H_2O$), prepared with a 1.00 mM solution of [**1**][TFA]$_2$, to a 1.00 mM solution of [**1**][TFA]$_2$.

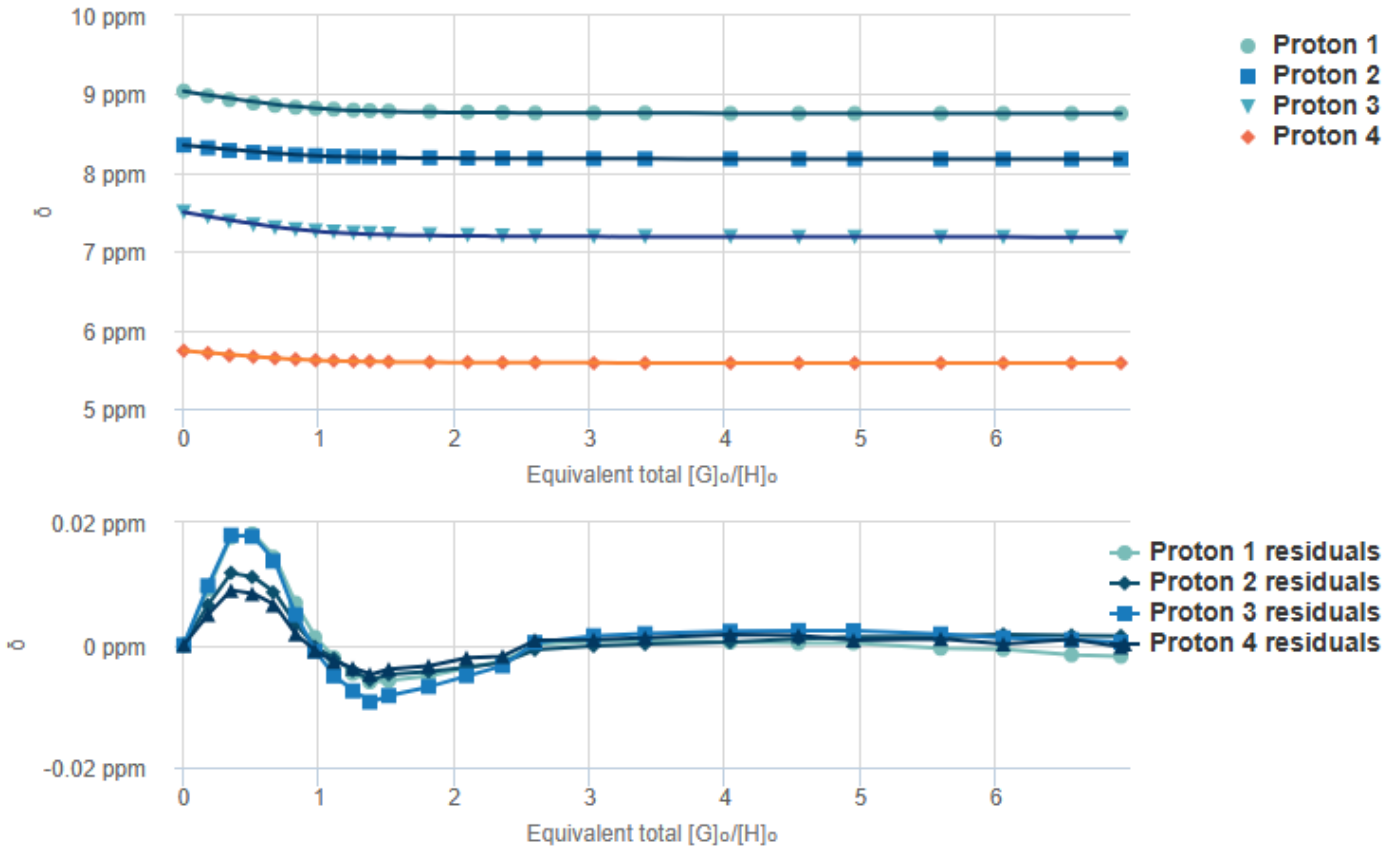

Details

Time to fit	0.2673 s
SSR	3.2488e-3
Fitted datapoints	96
Fitted params	5

Parameters

Parameter (bounds)	Optimised	Error	Initial
K (0 → ∞)	14507.13 M^{-1}	± 9.0131 %	100.00 M^{-1}

Figure S23. Nonlinear least-squares analysis of the ^{1}H NMR binding data (**Figure S22**) corresponding to the formation of [$\mathbf{1}^{2+}\supset TSP^{4-}$][$Na^{+}$]$_2$ complex. The data were fitted to a 1:1 (host:guest) binding model. The residual distribution is shown below the binding isotherm. The titration zero point was calculated from the fiiting curve. All solid lines were obtained from non-linear curve-fitting using the http://supramolecular.org/ web applet. Link to saved fit: http://app.supramolecular.org/bindfit/view/aa6c4f74-2361-4d14-a1d8-9896044f11ac.

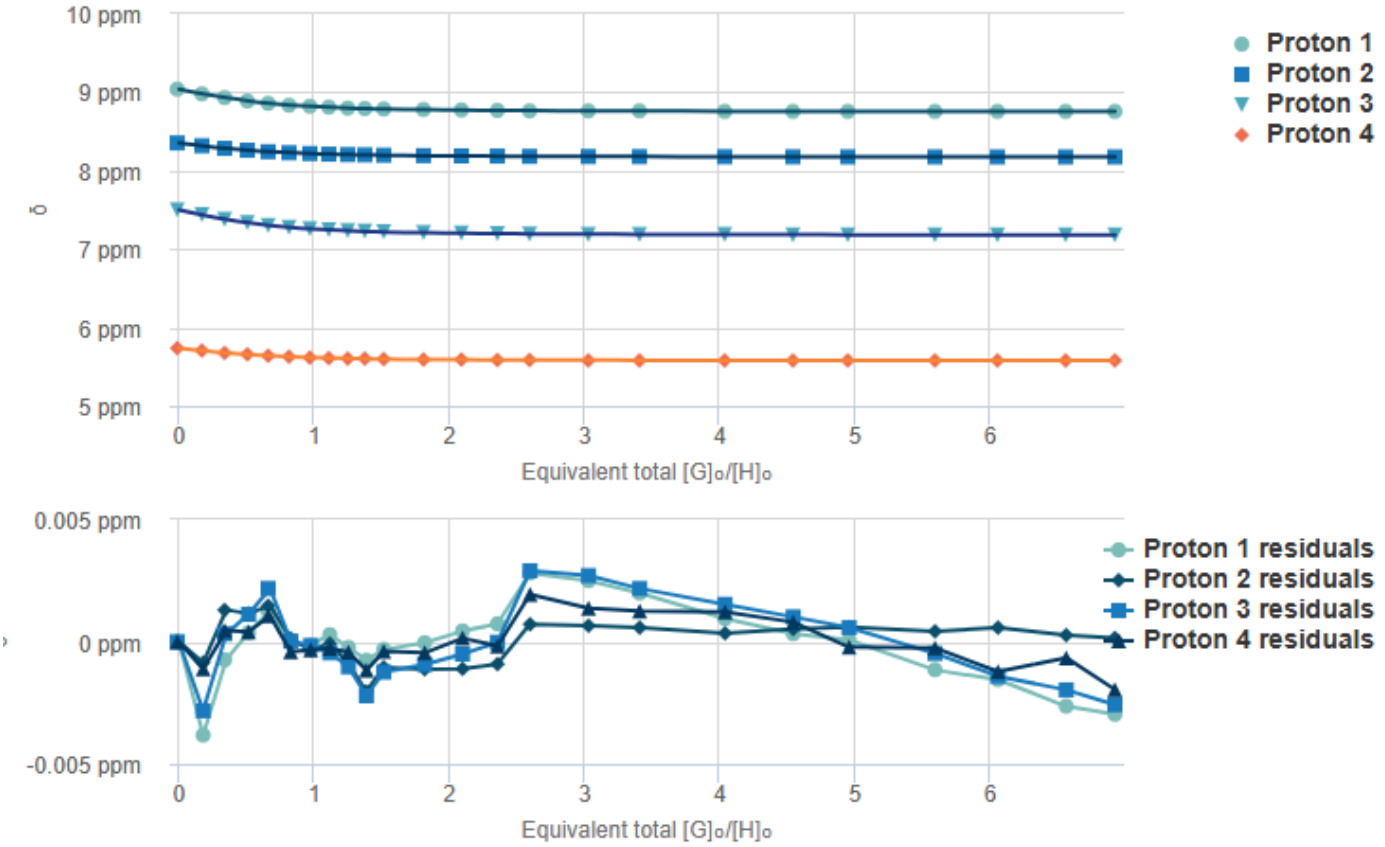

Details

Time to fit	1.6398 s
SSR	1.5525e-4
Fitted datapoints	96
Fitted params	10

Parameters

Parameter (bounds)	Optimised	Error	Initial
K_{11} (0 → ∞)	7387.90 M^{-1}	± 3.2281 %	1000.00 M^{-1}
K_{21} (0 → ∞)	326.79 M^{-1}	± 6.3927 %	100.00 M^{-1}

Figure S24. Nonlinear least-squares analysis of the ^{1}H NMR binding data (**Figure S22**) corresponding to the formation of [**1**$^{2+}$⊃TSP^{4-}][Na$^+$]$_2$ and [(**1**$^{2+}$)$_2$⊃TSP^{4-}][Na$^+$]$_4$ complexes. The data were fitted to a 2:1 (host:guest) binding model. The residual distribution is shown below the binding isotherm. The titration zero point was calculated from the fiiting curve. All solid lines were obtained from non-linear curve-fitting using the http://supramolecular.org/ web applet. Link to saved fit: http://app.supramolecular.org/bindfit/view/11caa373-7d58-4a60-9ea3-fa4e4efdf329.

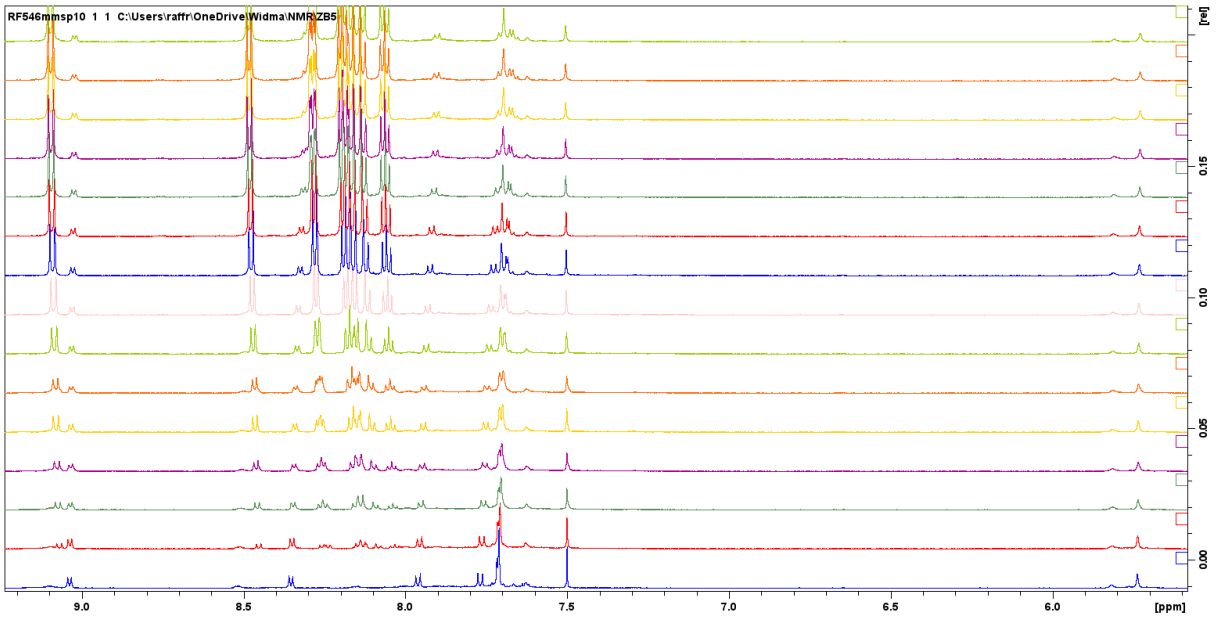

Figure S25. ^{1}H NMR titration spectra (600 MHz, 10% D_2O in DMSO-d_6, 300 K) obtained upon addition of 0–10.22 equiv. of a 13.40 mM solution of Na[**PMS**$^{-}$]), prepared with a 1.00 mM solution of [**1**][TFA]$_2$, to a 1.00 mM solution of [**1**][TFA]$_2$.

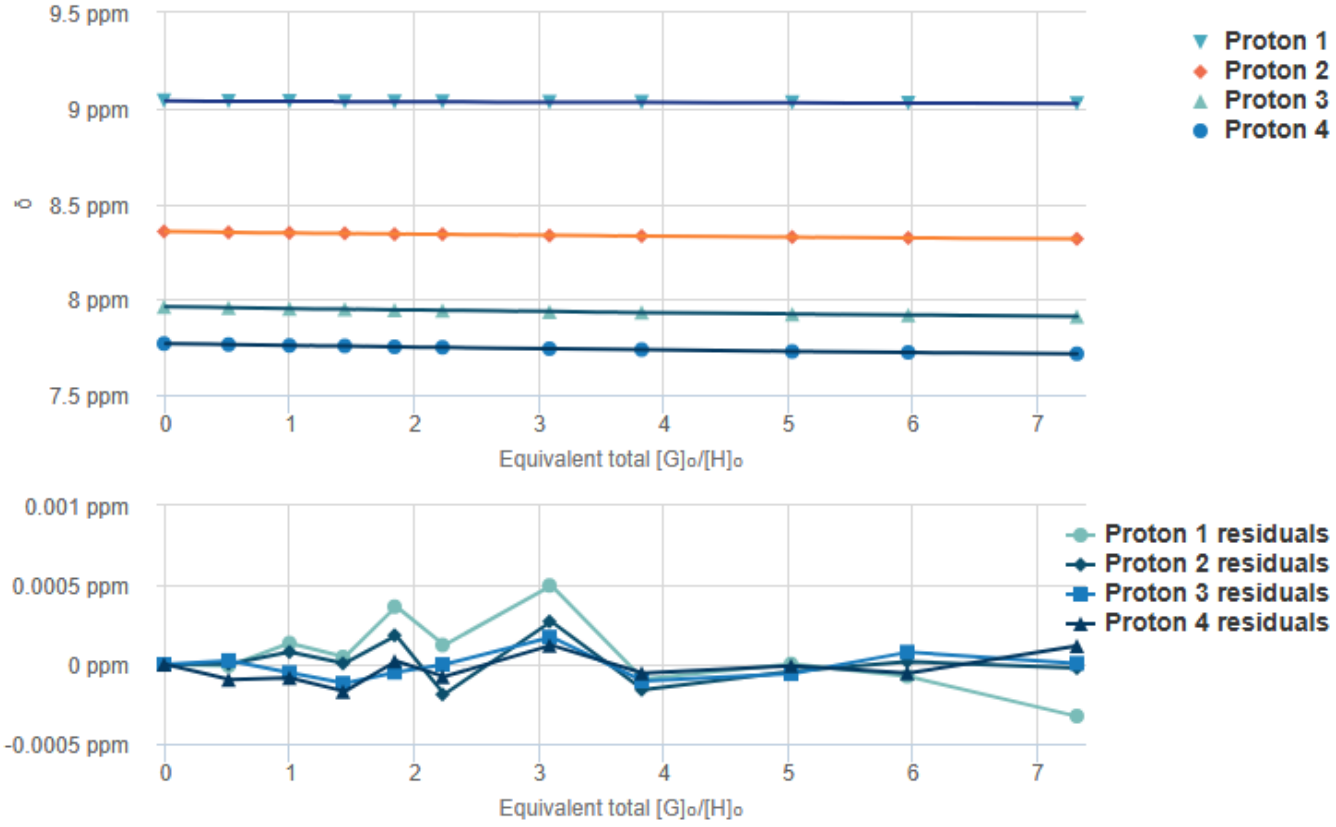

Details

Time to fit	0.2296 s
SSR	8.6644e-7
Fitted datapoints	44
Fitted params	5

Parameters

Parameter (bounds)	Optimised	Error	Initial
K (0 → ∞)	55.05 M^{-1}	± 0.2636 %	100.00 M^{-1}

Figure S26. Nonlinear least-squares analysis of the ^{1}H NMR binding data (**Figure S25**) corresponding to the formation of [**1**$^{2+}$⊃ **PMS**$^{-}$][TFA] complex. The data were fitted to a 1:1 (host:guest) binding model. The residual distribution is shown below the binding isotherm. All solid lines were obtained from non-linear curve-fitting using the http://supramolecular.org/ web applet. Link to saved fit: http://app.supramolecular.org/bindfit/view/27bf4520-c84a-45d1-b008-dc36dc9667bc.

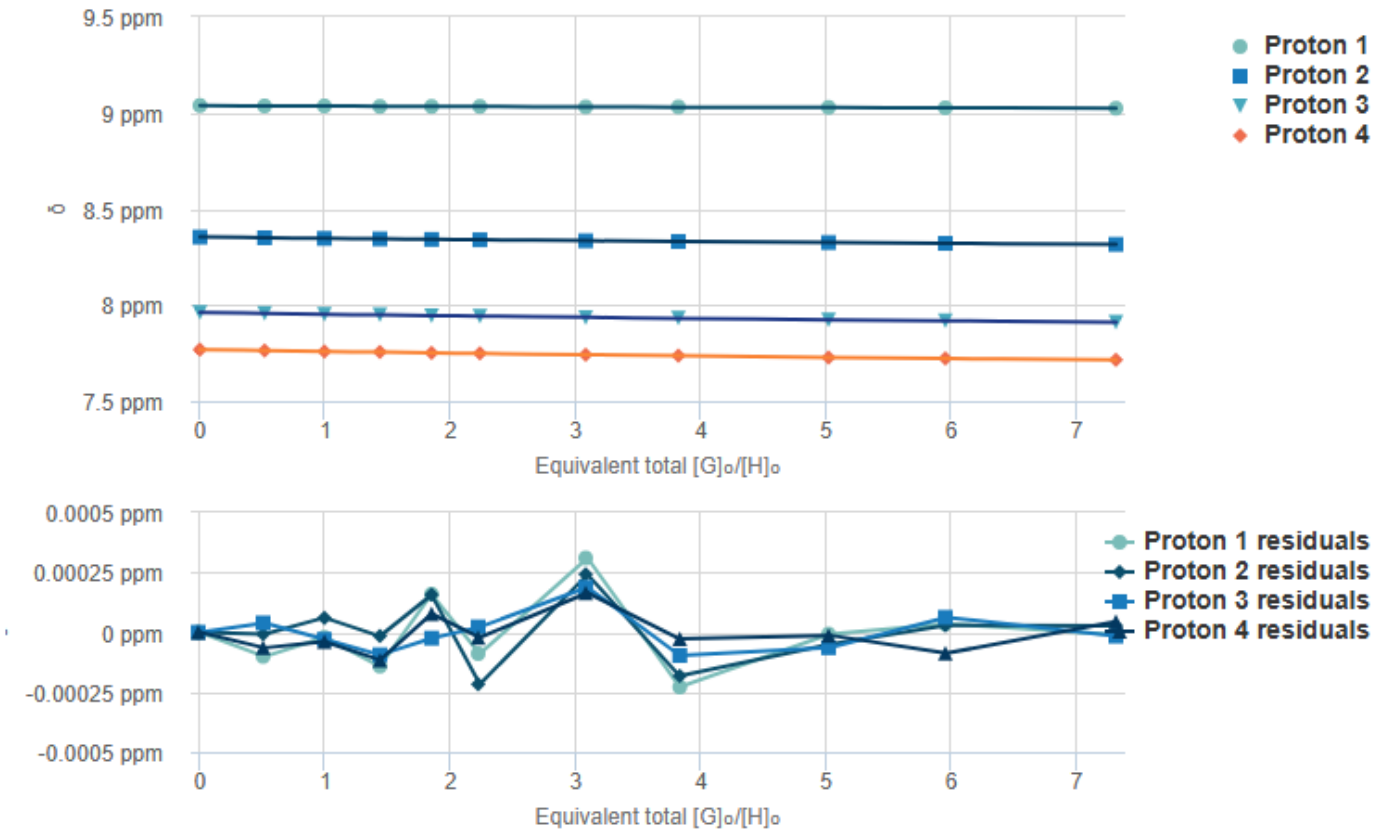

Details

Time to fit	1.4356 s
SSR	5.1359e-7
Fitted datapoints	44
Fitted params	10

Parameters

Parameter (bounds)	Optimised	Error	Initial
K_{11} (0 → ∞)	177.12 M^{-1}	± 0.8512 %	1000.00 M^{-1}
K_{12} (0 → ∞)	36.85 M^{-1}	± 1.7251 %	100.00 M^{-1}

Figure S27. Nonlinear least-squares analysis of the ^{1}H NMR binding data (**Figure S25**) corresponding to the formation of [$\mathbf{1}^{2+}\supset\mathbf{PMS}^-$][TFA] and [$\mathbf{1}^{2+}\supset(\mathbf{PMS}^-)_2$] complexes. The data were fitted to a 1:2 (host:guest) binding model. The residual distribution is shown below the binding isotherm. All solid lines were obtained from non-linear curve-fitting using the http://supramolecular.org/ web applet. Link to saved fit: http://app.supramolecular.org/bindfit/view/0932ffc8-e52d-4eed-b291-ff5182fcbed4.

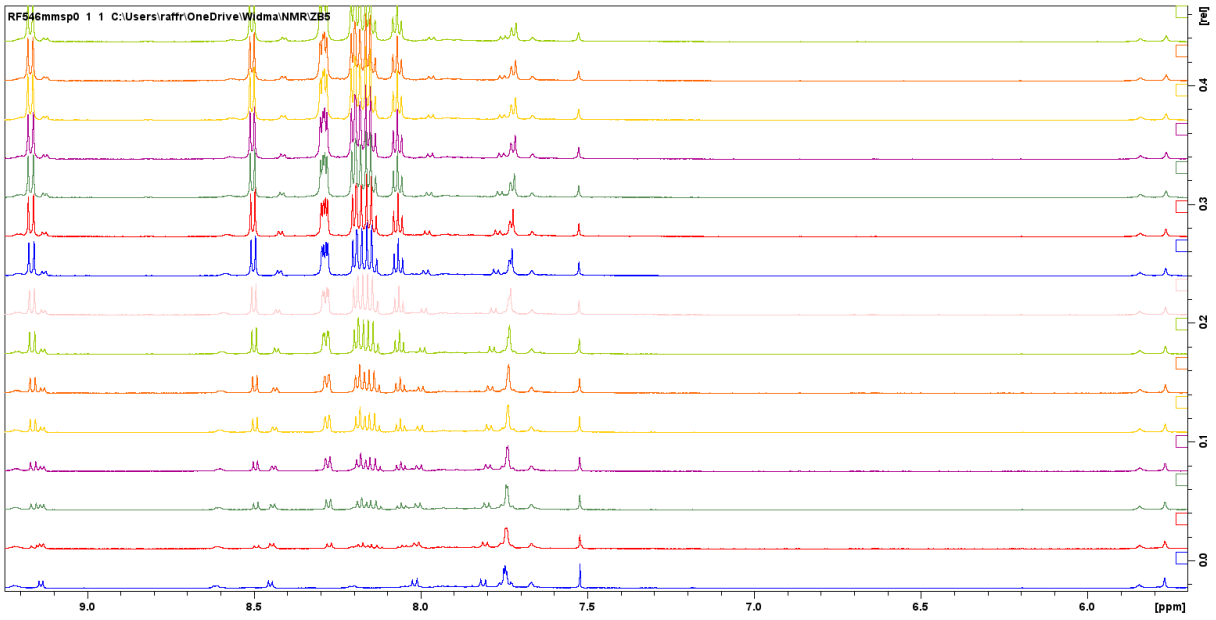

Figure S28. ^{1}H NMR titration spectra (600 MHz, DMSO-d_6, 300 K) obtained upon addition of 0–11.50 equiv. of a 15.10 mM solution of Na[**PMS**$^{-}$]), prepared with a 1.00 mM solution of [**1**][TFA]$_2$, to a 1.00 mM solution of [**1**][TFA]$_2$.

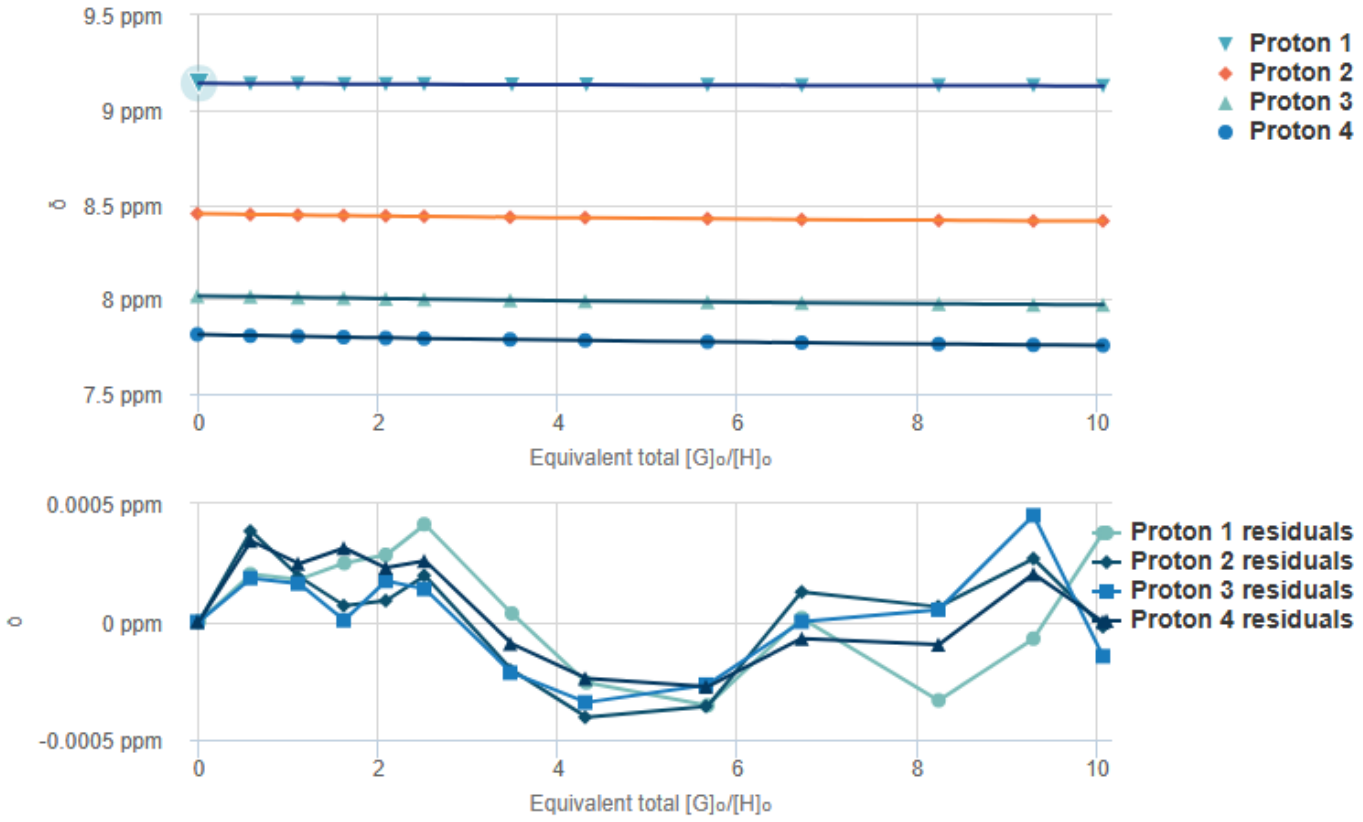

Details

Time to fit	0.2121 s
SSR	2.6577e-6
Fitted datapoints	52
Fitted params	5

Parameters

Parameter (bounds)	Optimised	Error	Initial
K (0 → ∞)	80.17 M^{-1}	± 0.4174 %	100.00 M^{-1}

Figure S29. Nonlinear least-squares analysis of the ^{1}H NMR binding data (**Figure S28**) corresponding to the formation of [**1**$^{2+}$⊃**PMS**$^{-}$][TFA] complex. The data were fitted to a 1:1 (host:guest) binding model. The residual distribution is shown below the binding isotherm. The titration zero point was calculated from the fiiting curve. All solid lines were obtained from non-linear curve-fitting using the http://supramolecular.org/ web applet. Link to saved fit: http://app.supramolecular.org/bindfit/view/ef6a7eaf-8542-48b0-87b4-7d3fe5a78f50.

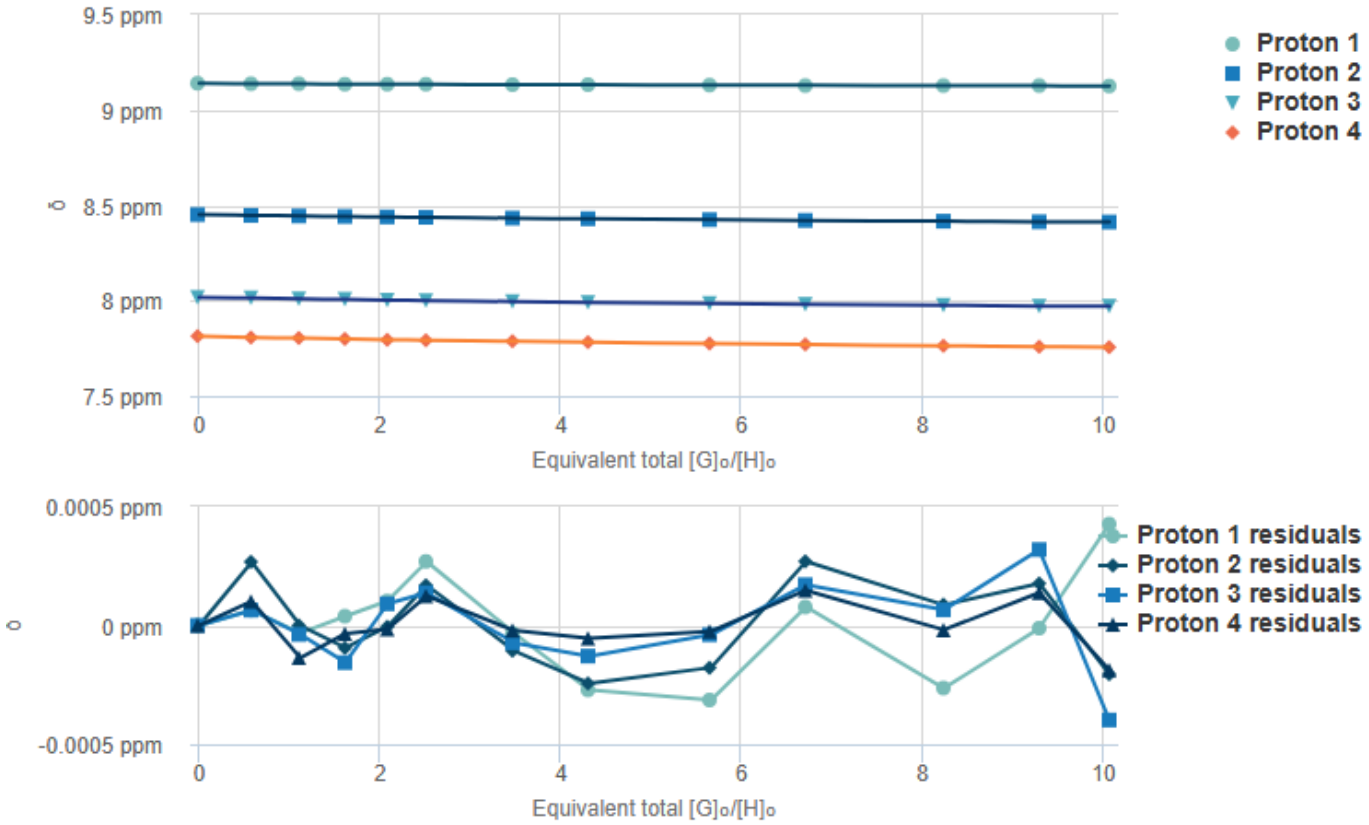

Details

Time to fit	1.3367 s
SSR	1.3846e-6
Fitted datapoints	52
Fitted params	10

Parameters

Parameter (bounds)	Optimised	Error	Initial
K_{11} (0 → ∞)	5601.54 M^{-1}	± 9.2162 %	100.00 M^{-1}
K_{12} (0 → ∞)	60.77 M^{-1}	± 0.5588 %	10.00 M^{-1}

Figure S30. Nonlinear least-squares analysis of the ^{1}H NMR binding data (**Figure S28**) corresponding to the formation of [**1**$^{2+}$⊃ **PMS**$^-$][X^-] and [**1**$^{2+}$⊃(**PMS**$^-$)$_2$] complexes. The data were fitted to a 1:2 (host:guest) binding model. The residual distribution is shown below the binding isotherm. The titration zero point was calculated from the fiiting curve. All solid lines were obtained from non-linear curve-fitting using the http://supramolecular.org/ web applet. Link to saved fit: http://app.supramolecular.org/bindfit/view/a00f35e8-05f2-48ac-8e71-0f0711011e07.

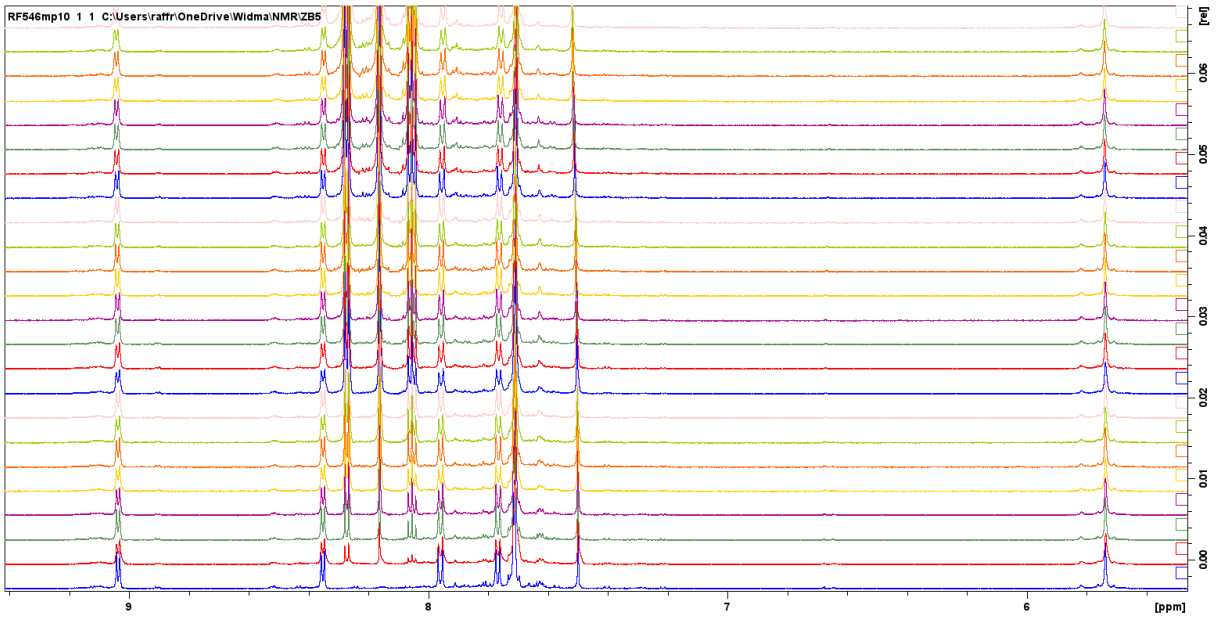

Figure S31. ^{1}H NMR titration spectra (600 MHz, 10% D_2O in DMSO-d_6, 300 K) obtained upon addition of 0–12.07 equiv. of a 15.85 mM solution of **P**, prepared with a 1.00 mM solution of [**1**][TFA]$_2$, to a 1.00 mM solution of [**1**][TFA]$_2$.

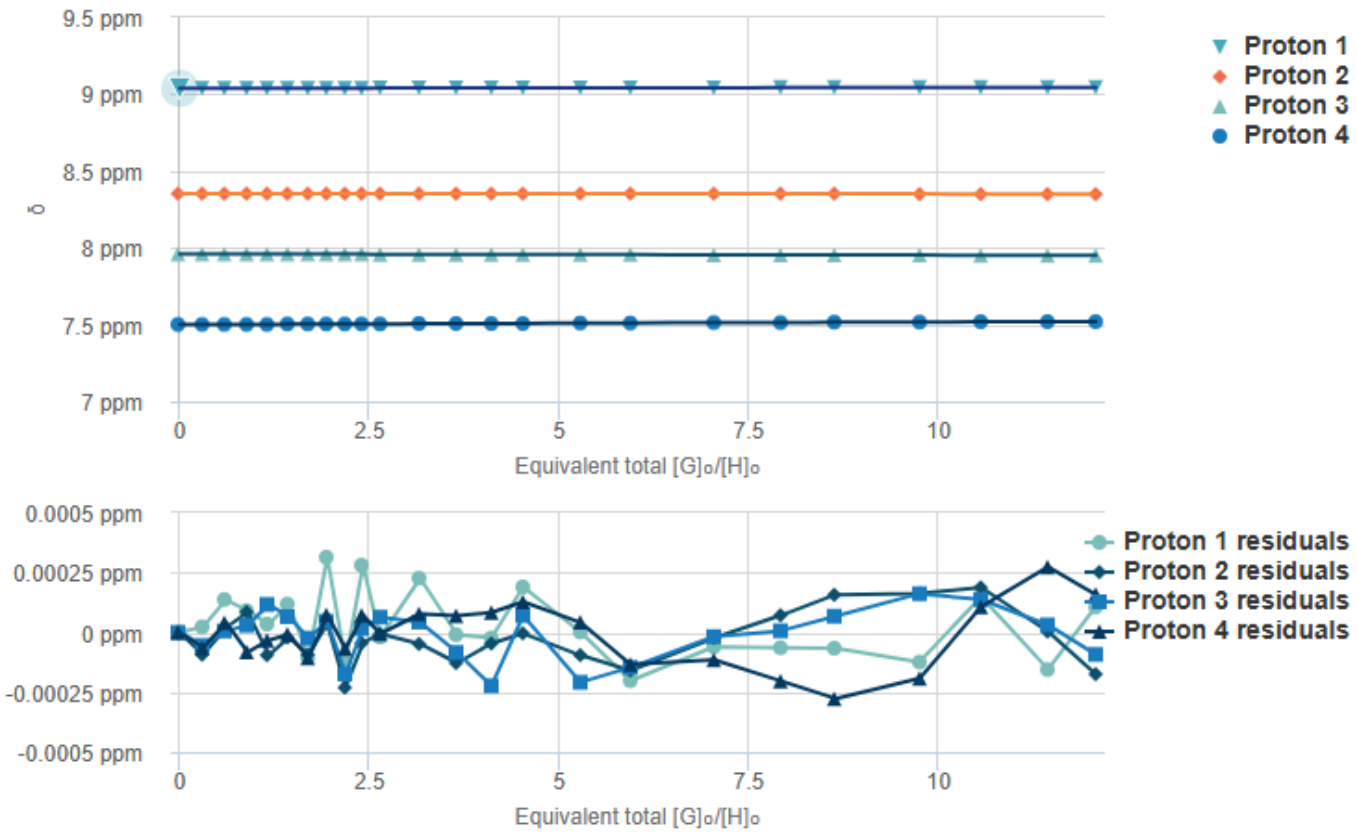

Details

Time to fit	0.2615 s
SSR	1.3491e-6
Fitted datapoints	96
Fitted params	5

Parameters

Parameter (bounds)	Optimised	Error	Initial
K (0 → ∞)	18.42 M^{-1}	± 0.4775 %	100.00 M^{-1}

Figure S32. Nonlinear least-squares analysis of the ^{1}H NMR binding data (**Figure S31**) corresponding to the formation of [**1**$^{2+}$⊃P][TFA]$_2$ complex. The data were fitted to a 1:1 (host:guest) binding model. The residual distribution is shown below the binding isotherm. All solid lines were obtained from non-linear curve-fitting using the http://supramolecular.org/ web applet. Link to saved fit: http://app.supramolecular.org/bindfit/view/99faf6d5-d320-449d-9001-444d51abed72.

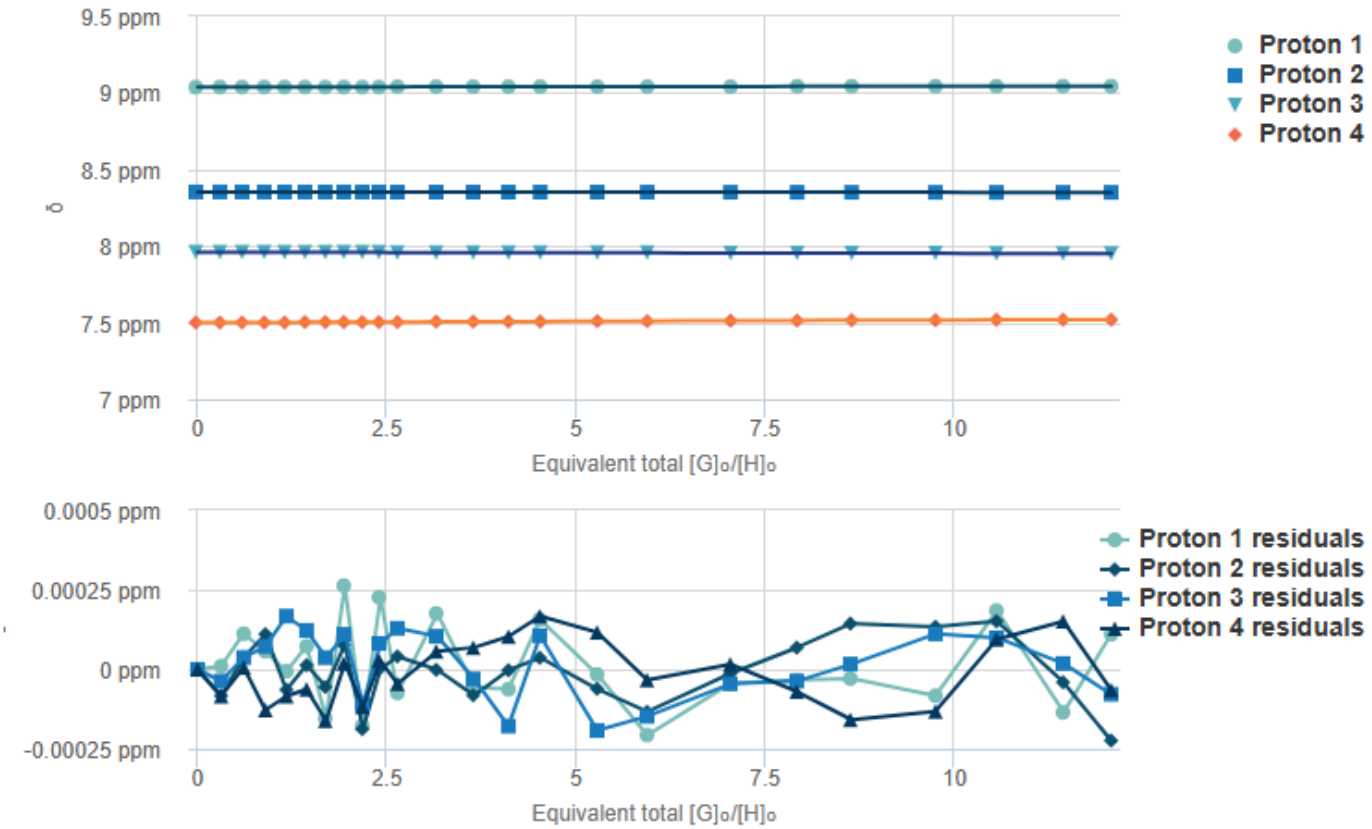

Details

Time to fit	2.0731 s
SSR	1.0684e-6
Fitted datapoints	96
Fitted params	10

Parameters

Parameter (bounds)	Optimised	Error	Initial
K_{11} (0 → ∞)	0.14 M^{-1}	± 0.8755 %	1000.00 M^{-1}
K_{12} (0 → ∞)	7072.91 M^{-1}	± 7.9328 %	100.00 M^{-1}

Figure S33. Nonlinear least-squares analysis of the ^{1}H NMR binding data (**Figure S31**) corresponding to the formation of [**1**$^{2+}$⊃P][TFA]$_2$ and [**1**$^{2+}$⊃(P)$_2$][TFA]$_2$ complexes. The data were fitted to a 1:2 (host:guest) binding model. The residual distribution is shown below the binding isotherm. All solid lines were obtained from non-linear curve-fitting using the http://supramolecular.org/ web applet. Link to saved fit: http://app.supramolecular.org/bindfit/view/5a0715f1-7d4c-42c1-8419-2c4276d43677.

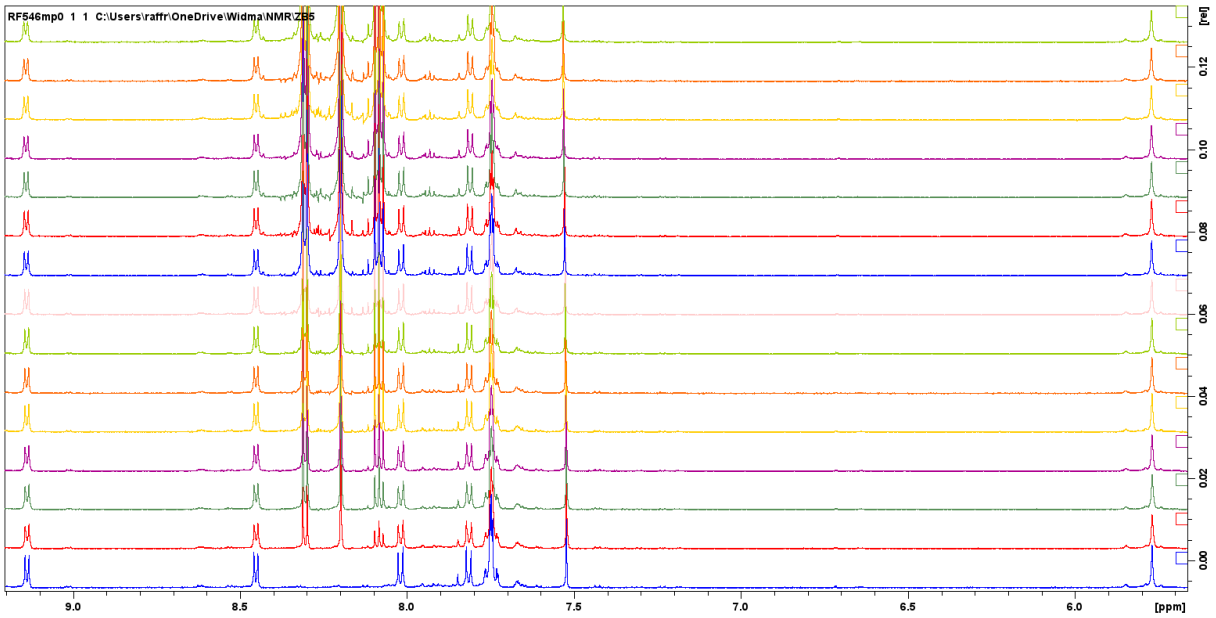

Figure S34. ^{1}H NMR titration spectra (600 MHz, DMSO-d_6, 300 K) obtained upon addition of 0–13.79 equiv. of a 15.08 mM solution of P, prepared with a 0.83 mM solution of [**1**][TFA]$_2$, to a 0.83 mM solution of [**1**][TFA]$_2$.

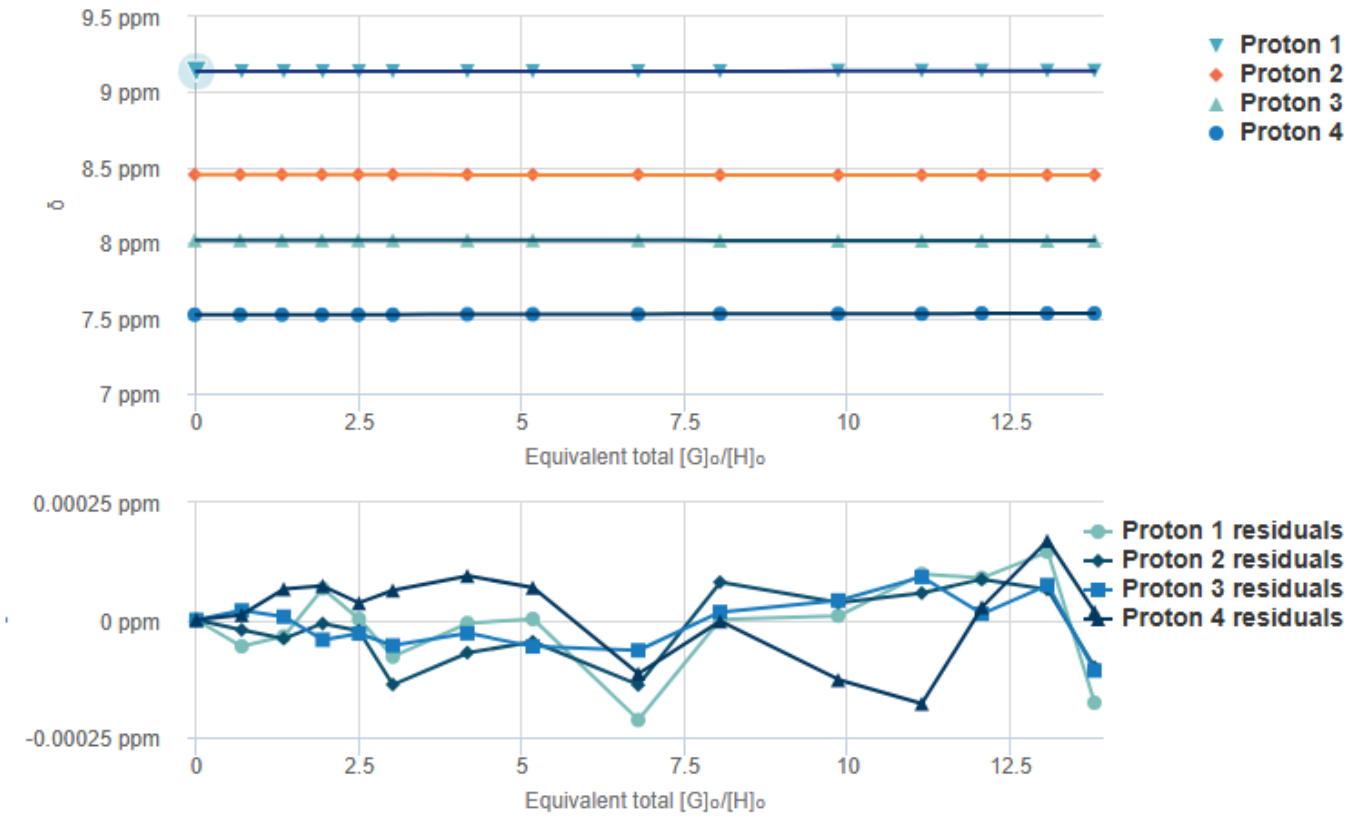

Details

Time to fit	0.8966 s
SSR	3.7210e-7
Fitted datapoints	60
Fitted params	5

Parameters

Parameter (bounds)	Optimised	Error	Initial
K (0 → ∞)	17.50 M^{-1}	± 0.7542 %	100.00 M^{-1}

Figure S35. Nonlinear least-squares analysis of the ^{1}H NMR binding data (**Figure S34**) corresponding to the formation of [**1**⊃P][TFA]$_2$ complex. The data were fitted to a 1:1 (host:guest) binding model. The residual distribution is shown below the binding isotherm. All solid lines were obtained from non-linear curve-fitting using the http://supramolecular.org/ web applet. Link to saved fit: http://app.supramolecular.org/bindfit/view/e33b8795-10f3-46f8-a92e-71f124de98fb.

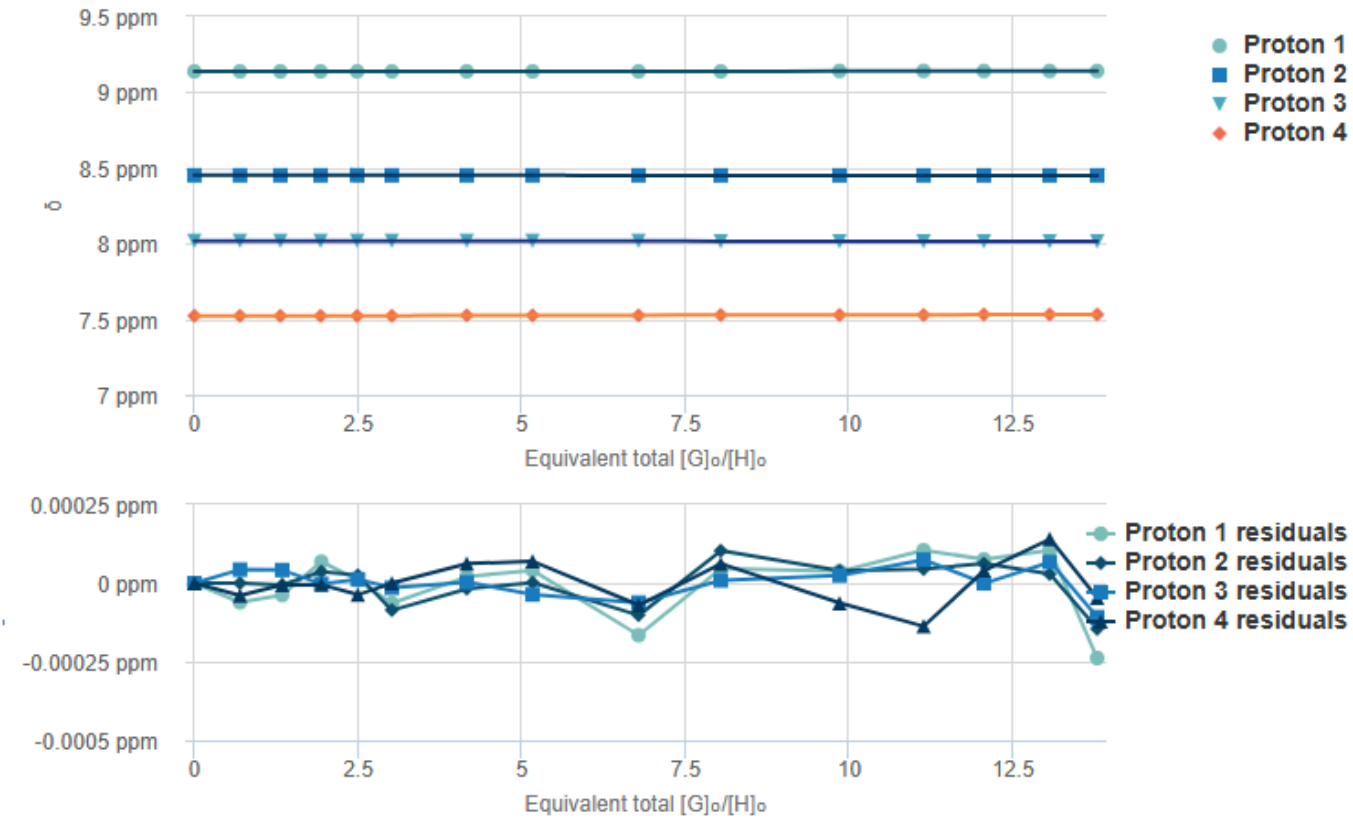

Details

Time to fit	1.1662 s
SSR	2.9028e-7
Fitted datapoints	60
Fitted params	10

Parameters

Parameter (bounds)	Optimised	Error	Initial
K_{11} (0 → ∞)	177.71 M^{-1}	± 4.9443 %	1000.00 M^{-1}
K_{12} (0 → ∞)	39.72 M^{-1}	± 3.8000 %	100.00 M^{-1}

Figure S36. Nonlinear least-squares analysis of the ^{1}H NMR binding data (**Figure S34**) corresponding to the formation of [**1**⊃P][TFA]$_2$ and [**1**⊃(P)$_2$][TFA]$_2$ complexes. The data were fitted to a 1:2 (host:guest) binding model. The residual distribution is shown below the binding isotherm. All solid lines were obtained from non-linear curve-fitting using the http://supramolecular.org/ web applet. Link to saved fit: http://app.supramolecular.org/bindfit/view/a6bf2f40-1432-4912-a4d3-96a0761aec58.

4.3. Absorption Spectroscopy

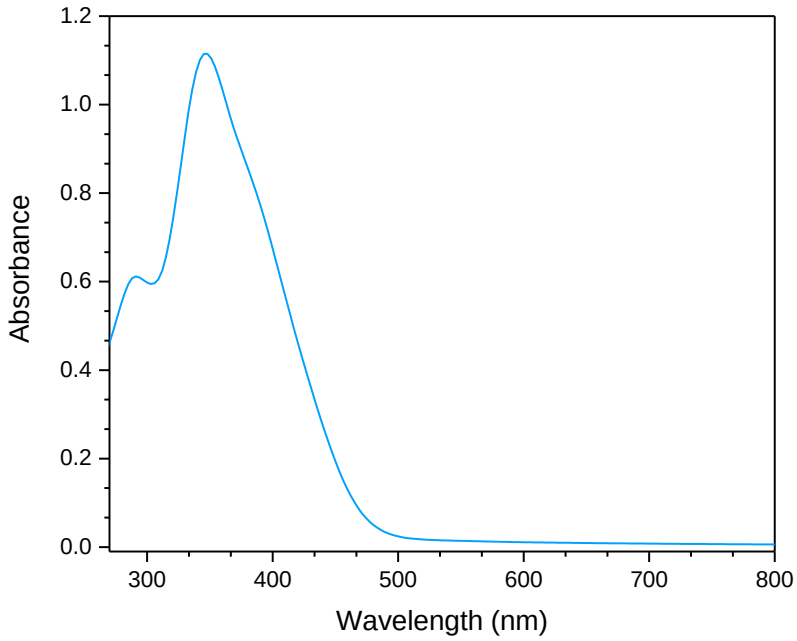

Figure S37. Absorption spectrum of compound [**1**][TFA]$_2$ in DMF.

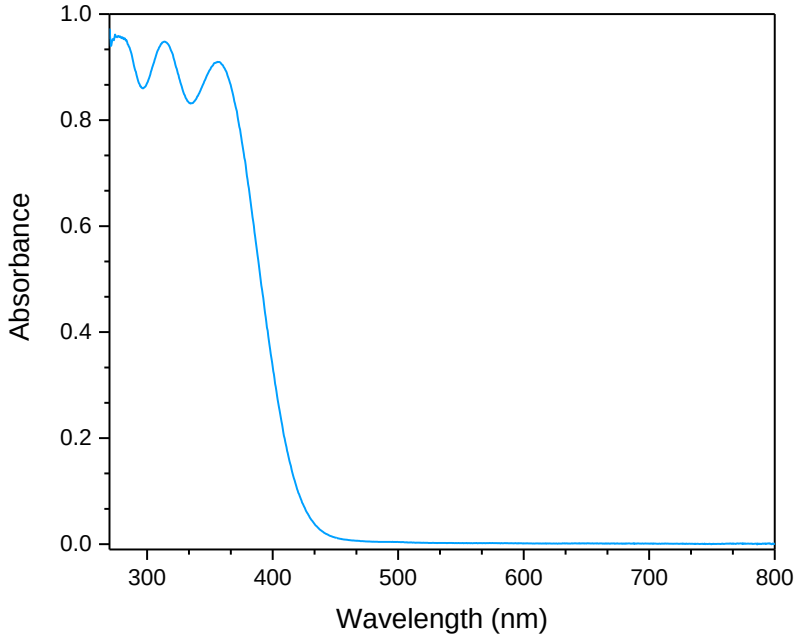

Figure S38. Absorption spectrum of compound [**2**][TFA]$_2$ in DMF.

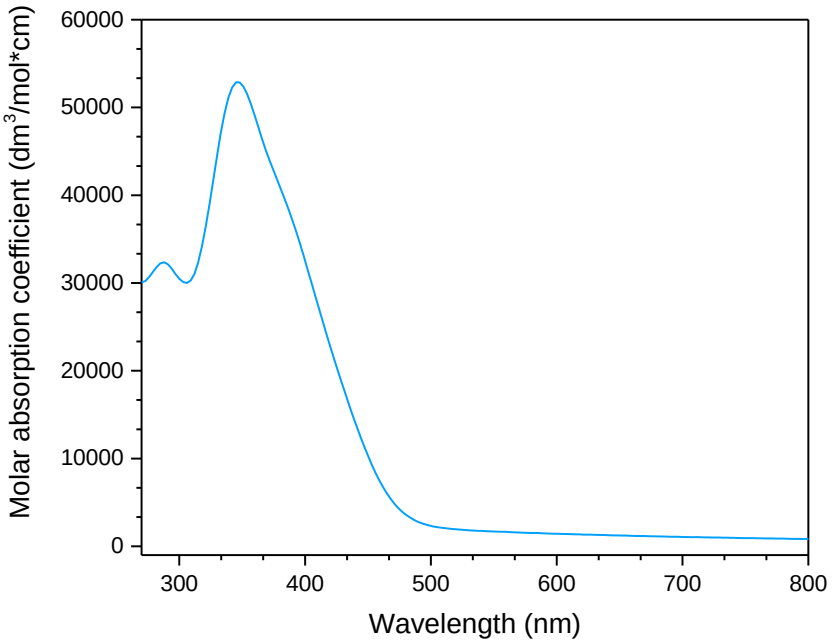

Figure S39. Absorption spectrum of compound [**1**][TFA]$_2$ in DMF.

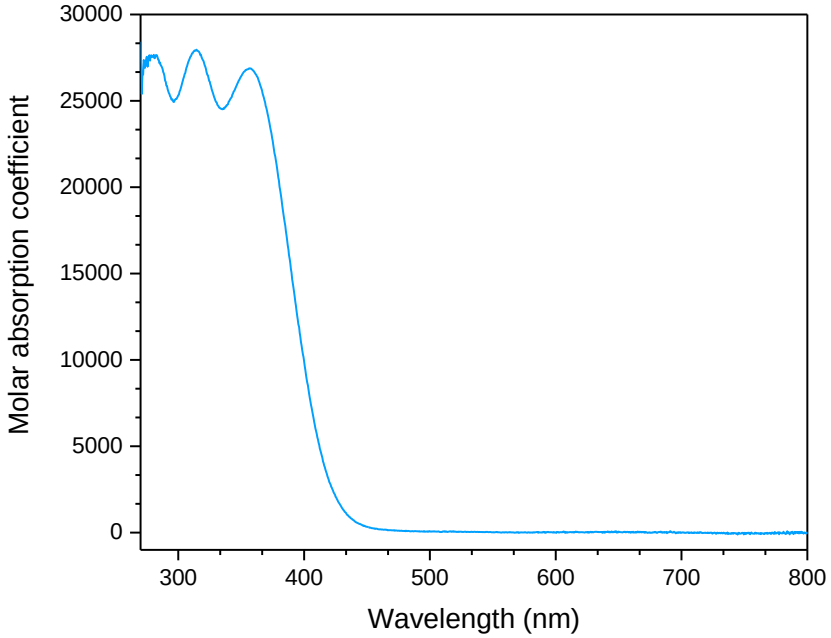

Figure S40. Absorption spectrum of compound [**2**][TFA]$_2$ in DMF.

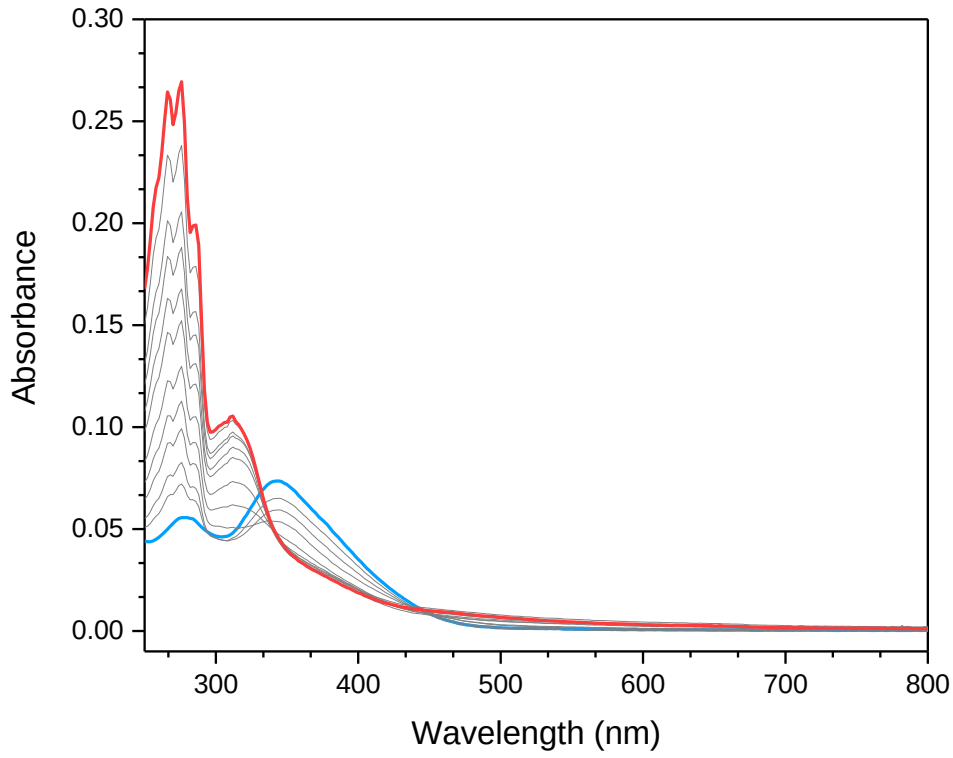

Figure S41. Titration of [**1**][TFA]$_2$ (0.019 mM in THF) with sodium anthracenide.

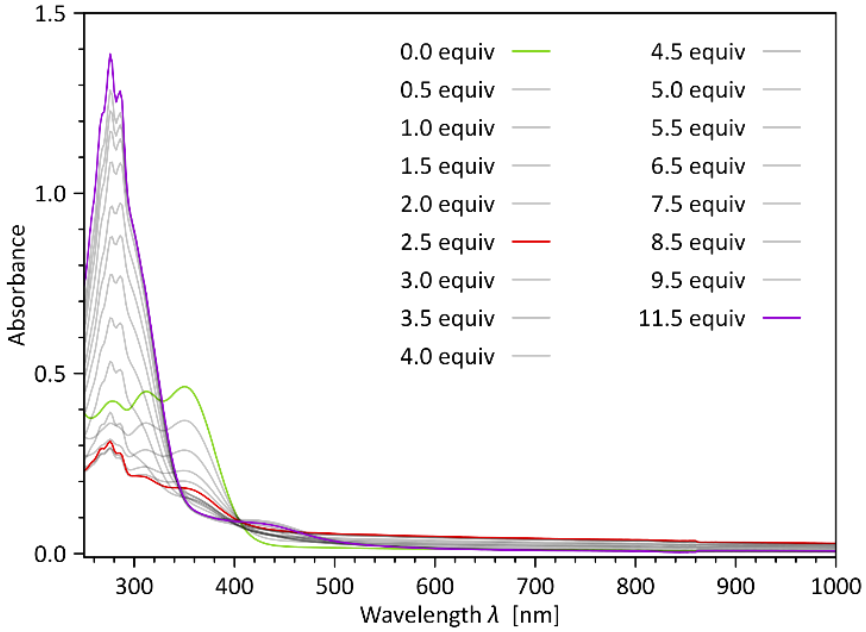

Figure S42. Titration of [**2**][TFA]$_2$ (0.027 mM in THF) with sodium anthracenide.

4.4. Emission Spectroscopy

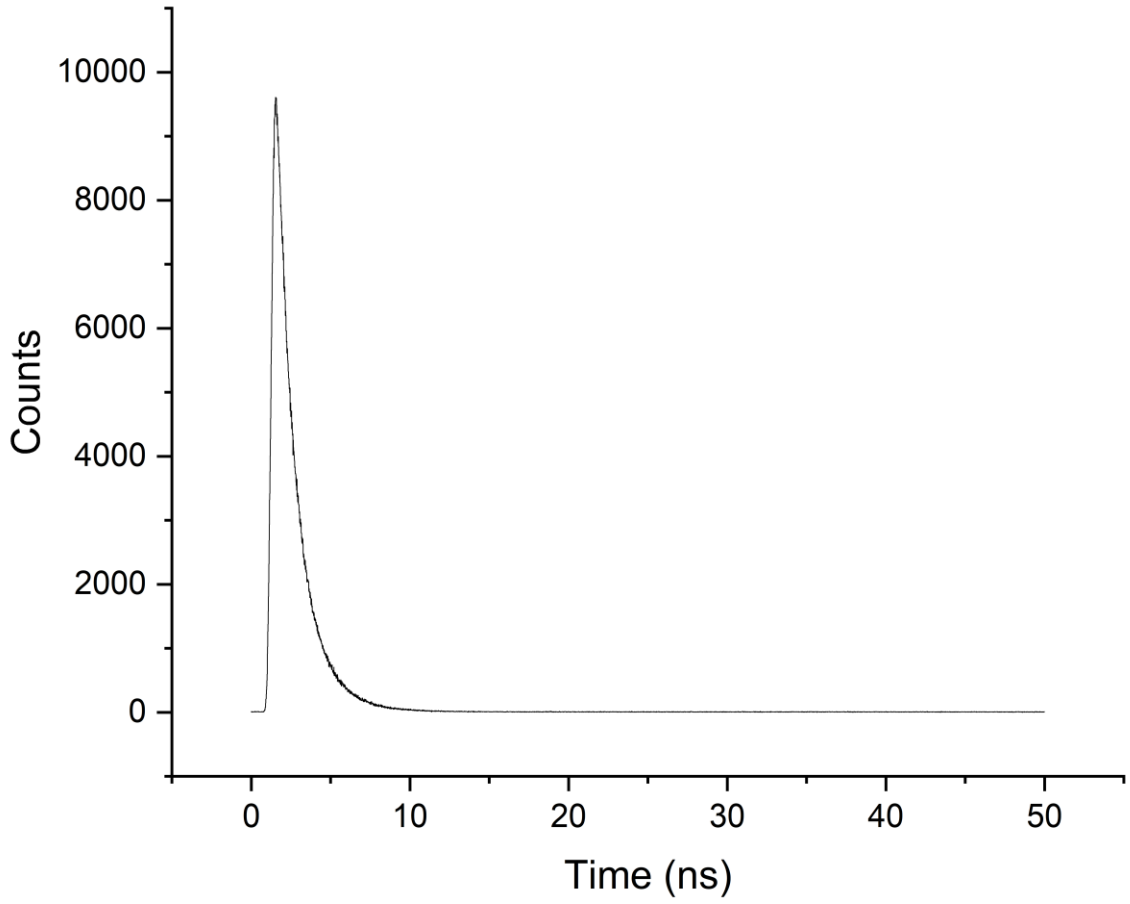

Figure S43. Fluorescence decay traces of [**1**][TFA]$_2$ in DMF (λ^{em} = 535 nm).

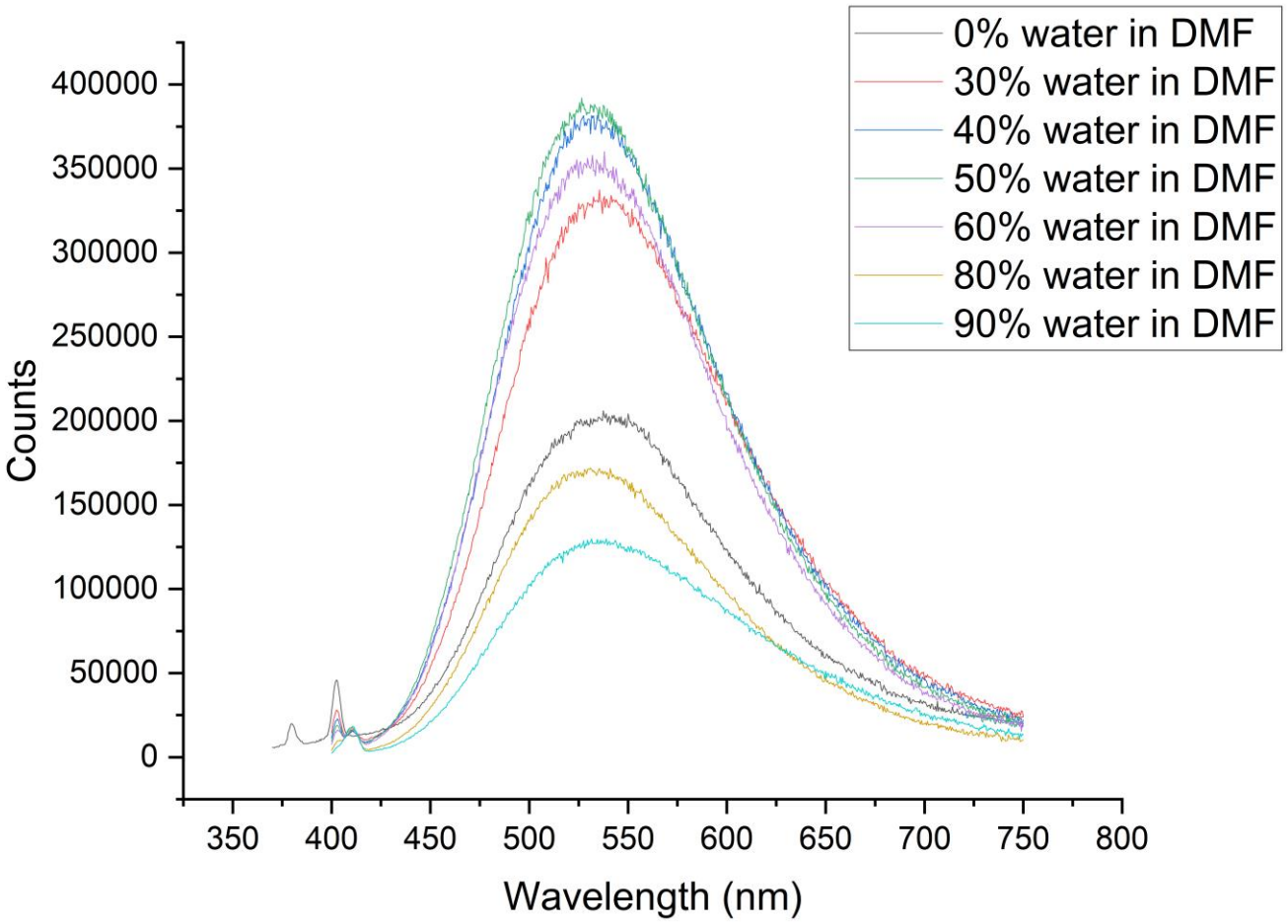

Figure S44. Emission spectra of [**1**][TFA]$_2$ in a mixtures of water and DMF.

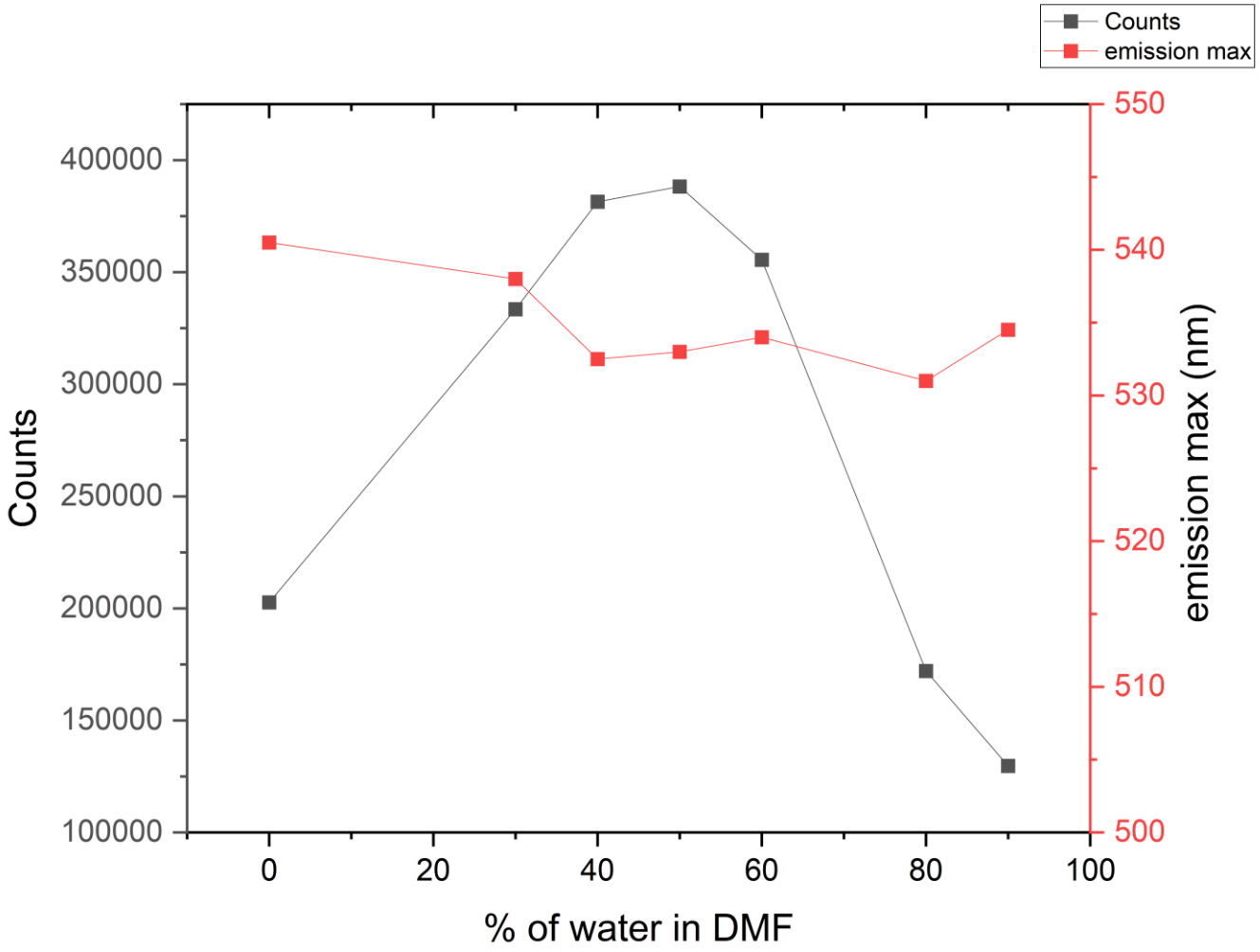

Figure S45. Number of counts and λ_{max}^{em} depending of a content of water in DMF.

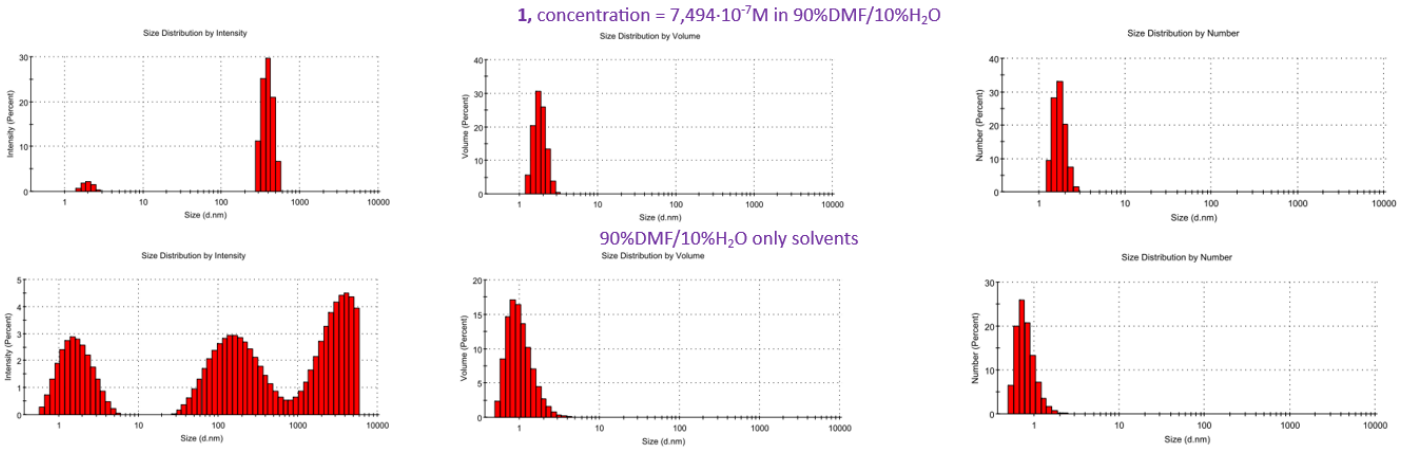

Figure S46. DLS measurements of a solution of [**1**][TFA]$_2$ in 10% water in DMF mixture (top) and pure solvent mixture (bottom).

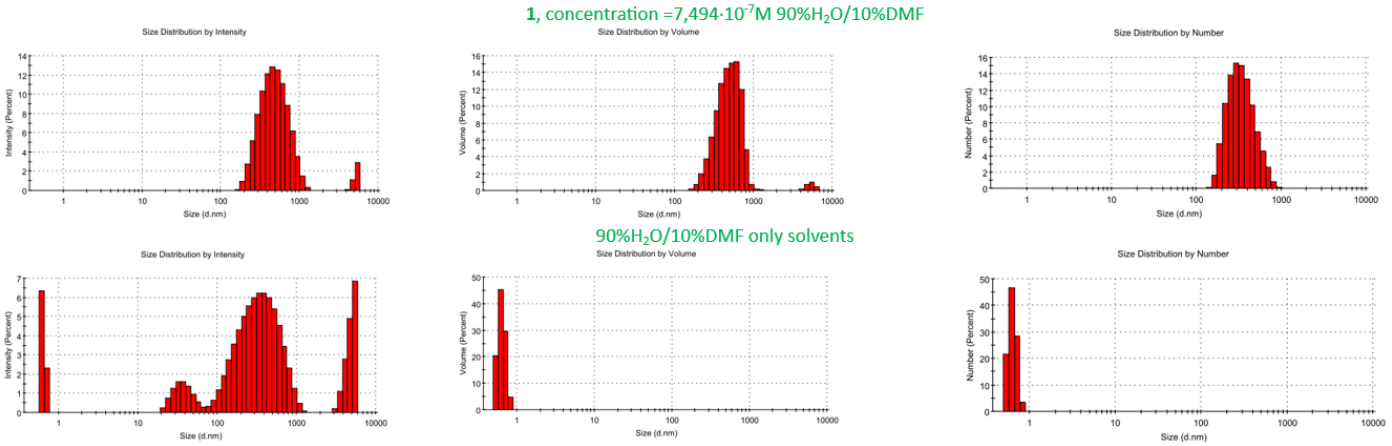

Figure S47. DLS measurements of a solution of [**1**][TFA]$_2$ in 90% water in DMF mixture (top) and pure solvent mixture (bottom).

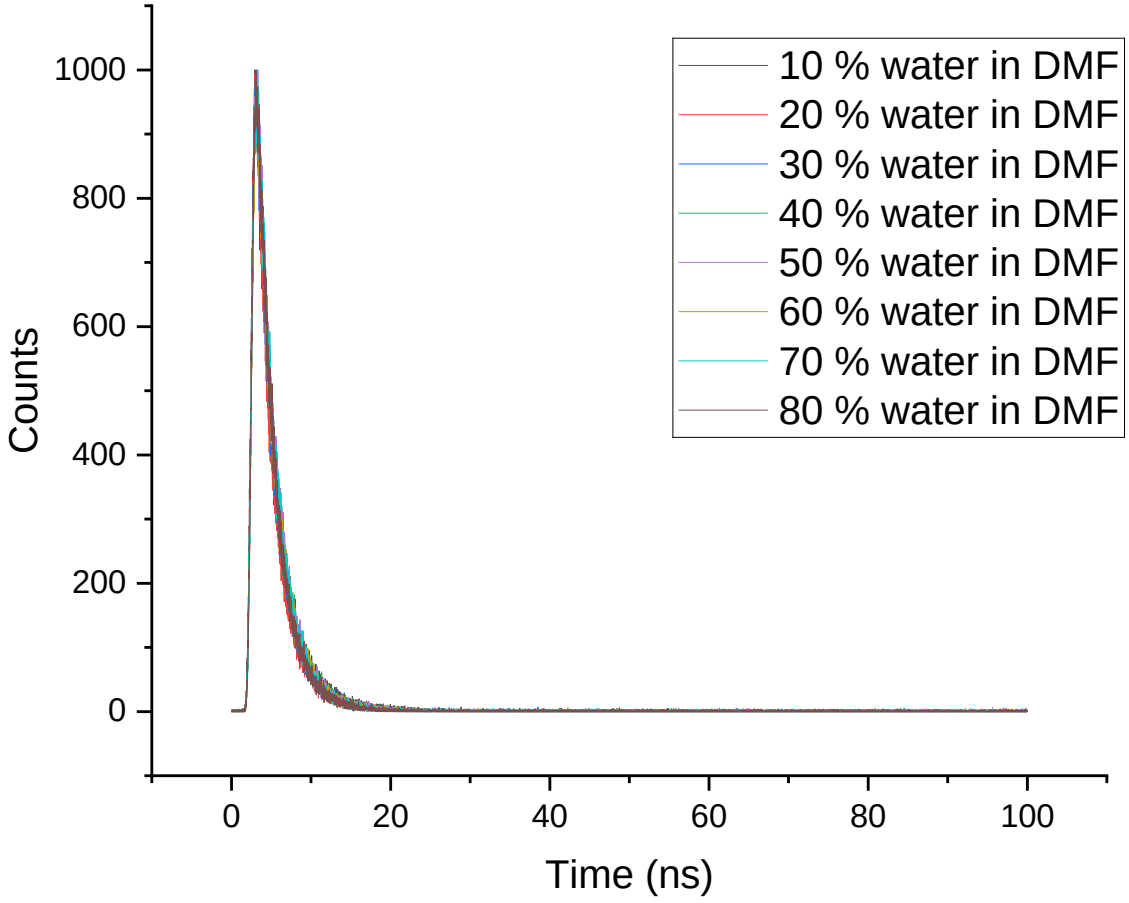

Figure S48. Fluorescence decay traces of [**1**][TFA]$_2$ in a mixtures of water and DMF (λ_{em} = 535 nm).

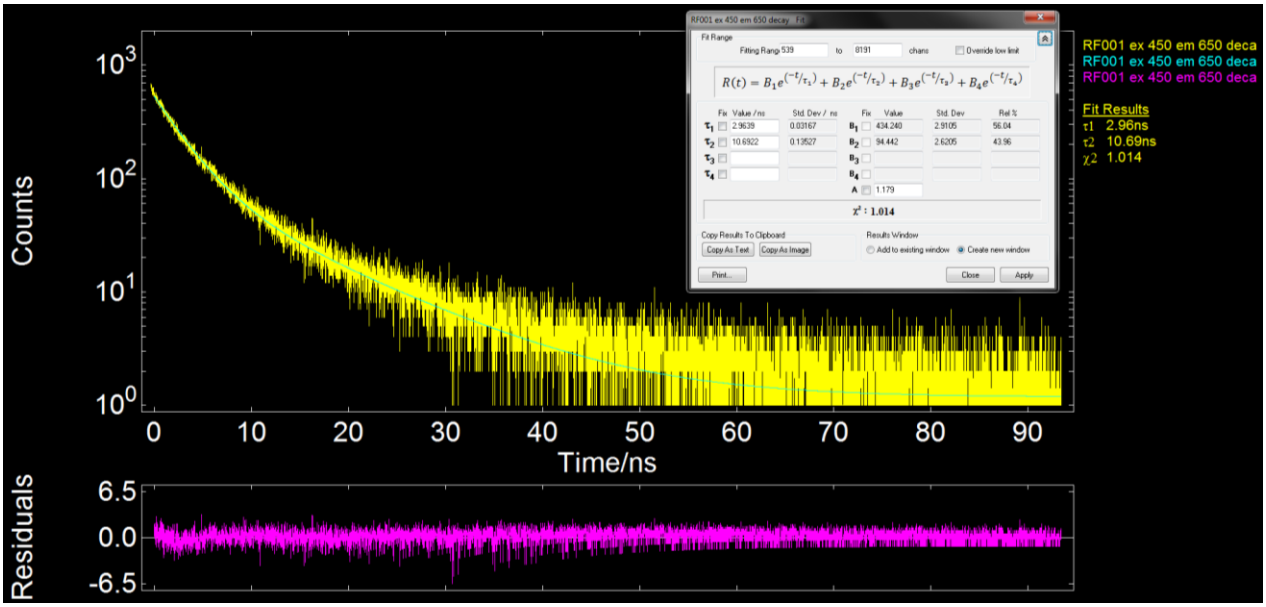

Figure S49. Fluorescence decay traces of solid state [**1**][TFA]$_2$ (λ_{em} = 650 nm).

4.5. Electrochemistry

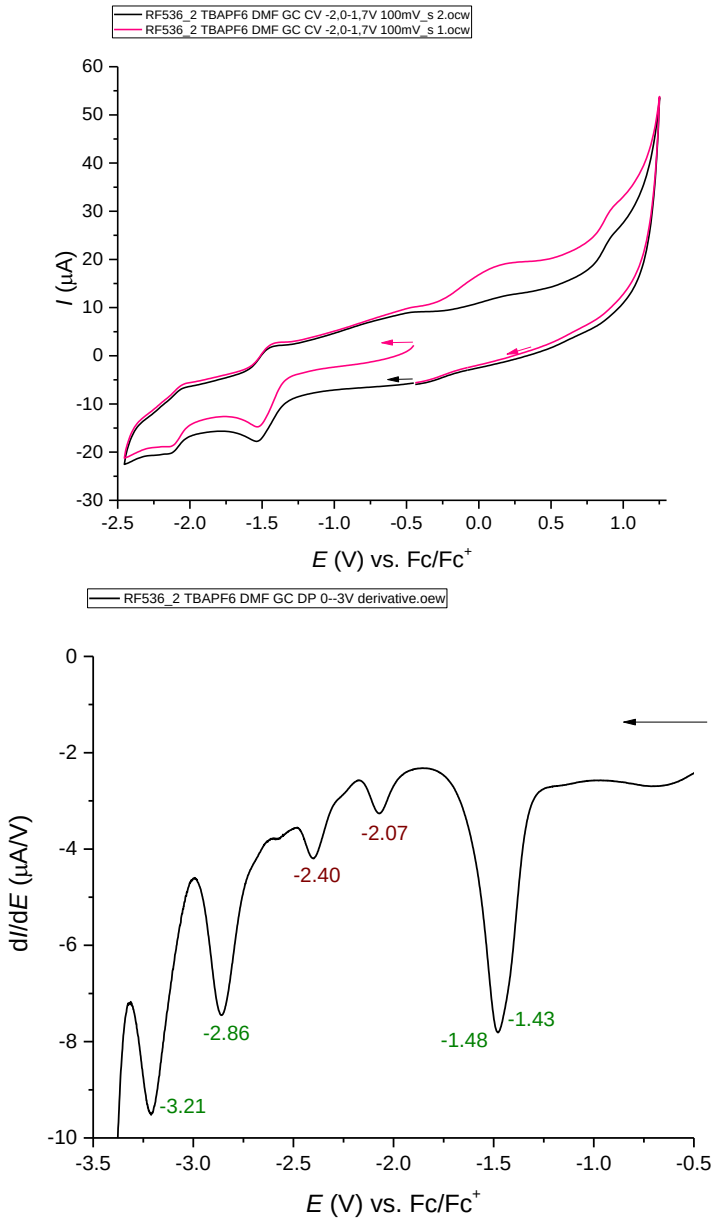

Figure S50. Differential pulse (bottom) and cyclic (top) voltammograms for [**1**][TFA]$_2$ in DMF. The green numbers are peak potentials in volts referenced with ferrocene/ferrocenium couple potential. The arrows indicate directions of the potential sweeps. Conditions: supporting electrolyte, [Bu$_4$N]PF$_6$; working electrode, glassy carbon; reference electrode, Ag/AgCl; auxiliary electrode, platinum rod.

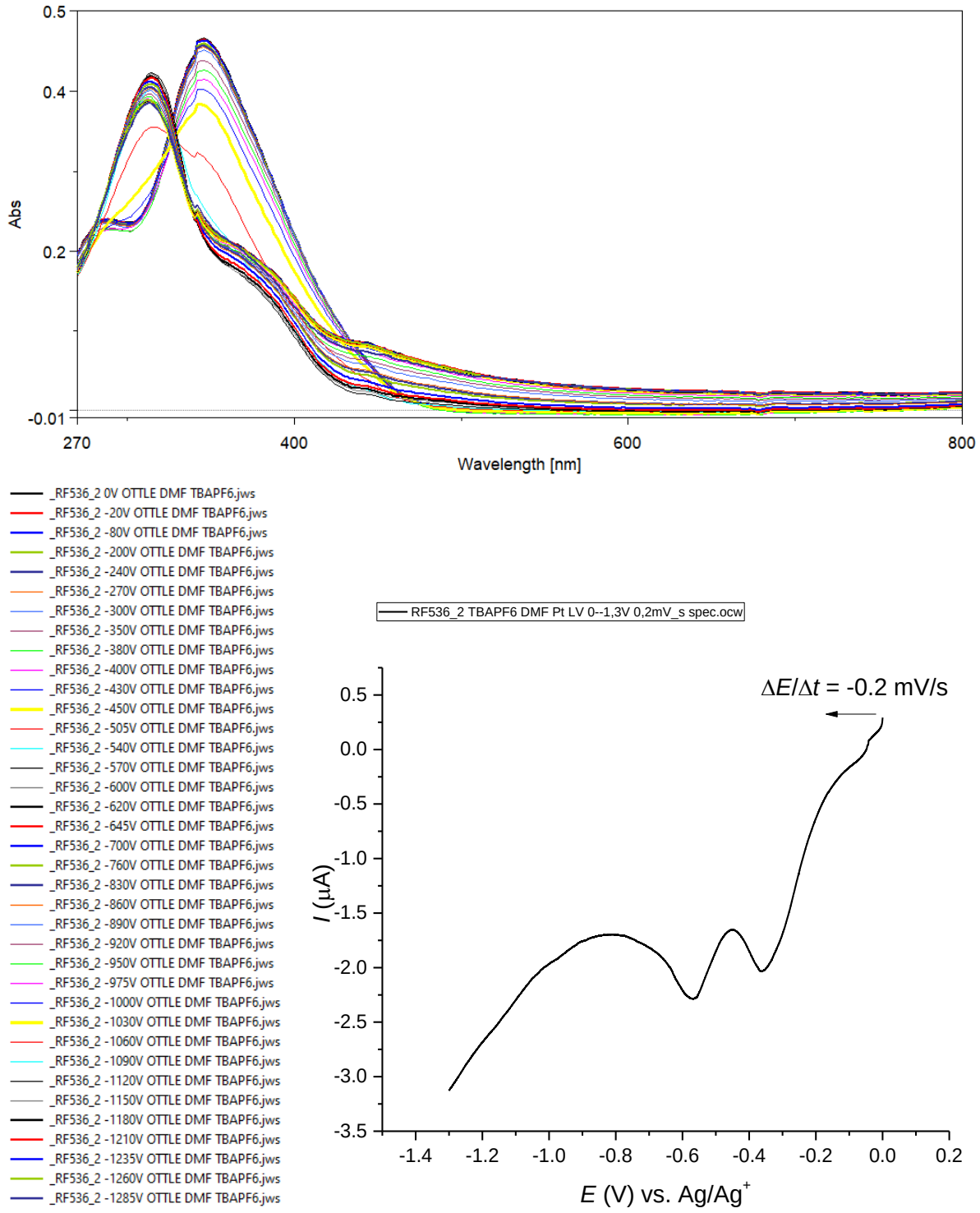

Figure S51. In-situ UV-Vis reduction of [**1**][TFA]$_2$ in TBAPF$_6$/DMF obtained by potential scanning vs. Ag/Ag$^+$.

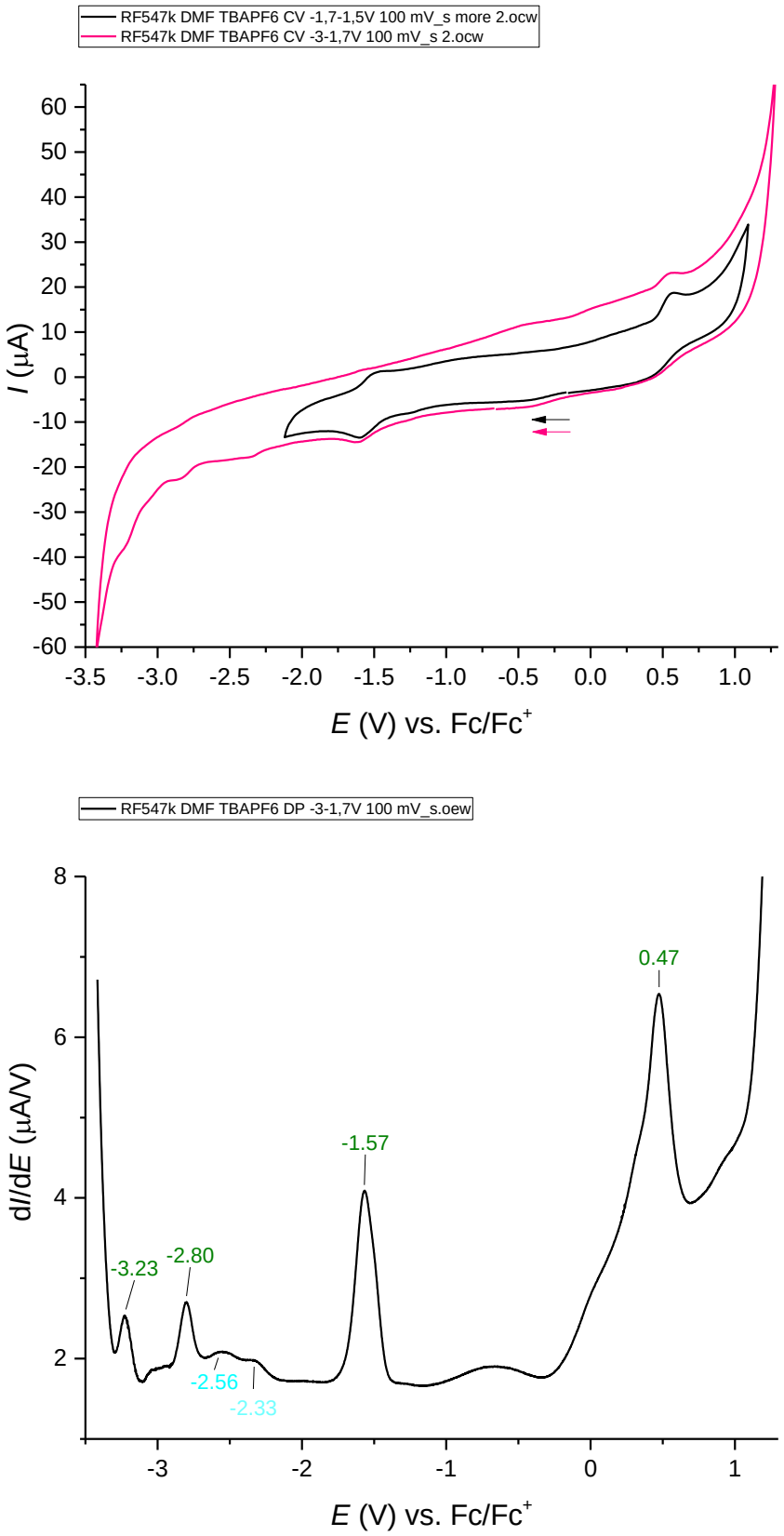

Figure S52. Differential pulse (bottom) and cyclic (top) voltammograms for [**2**][TFA]$_2$ in DMF. The green numbers are peak potentials in volts referenced with ferrocene/ferrocenium couple potential. The arrows indicate directions of the potential sweeps. Conditions: supporting electrolyte, $[Bu_4N]PF_6$; working electrode, glassy carbon; reference electrode, Ag/AgCl; auxiliary electrode, platinum rod.

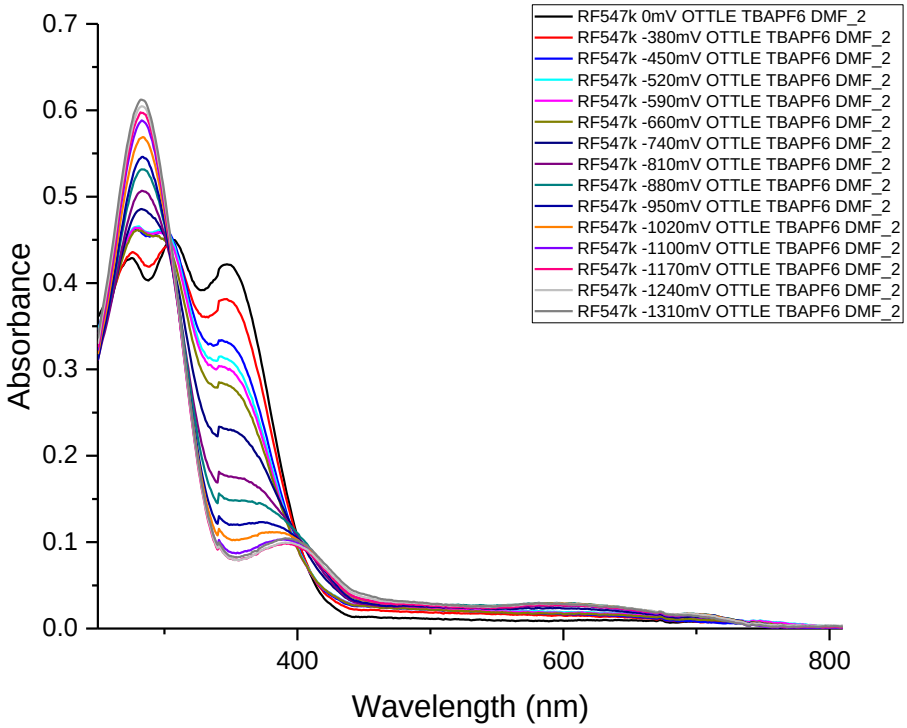

Figure S53. In-situ UV-Vis reduction of [**2**][TFA]$_2$ in TBAPF$_6$/DMF obtained by potential scanning vs. Ag/Ag$^+$.

5. Computational Data

5.1. Energies and Geometries

Table S1. Data for DFT-optimized stationary points discussed in this work (GD3BJ/CAM-B3LYP/6-31G(d,p)).

System[a]	n[b]	m[b]	SCF E[c]	ZPV[d]	LVF[e]	E[f]	H[f]	G[f]	$\langle S^2 \rangle$[g]	*.xyz[h]
			a.u.	a.u.	cm^{-1}	a.u.	a.u.	a.u.		
1	2	1	–2189.778812	0.798344	15.64	–2188.938879	–2188.937935	–2189.057390		1(2,1)
1	1	2	–2190.007029	0.794466	14.91	–2189.170548	–2189.169604	–2189.290431	0.75	1(1,2)
1	0	1	–2190.173638	0.790590	14.63	–2189.340523	–2189.339579	–2189.461085	0.80	1(0,1)
1	0	3	–2190.173635	0.790591	14.62	–2189.340519	–2189.339575	–2189.462119	2.01	1(0,3)
2	2	1	–2418.790803	0.864803	11.10	–2417.878873	–2417.877929	–2418.010041		2(2,1)
2	1	2	–2419.015364	0.860852	10.60	–2418.106925	–2418.105981	–2418.239762	0.75	2(1,2)
2	0	1	–2419.177348	0.856849	9.76	–2418.272403	–2418.271459	–2418.405936	0.75	2(0,1)
2	0	3	–2419.177347	0.856849	9.77	–2418.272402	–2418.271458	–2418.406970	2.01	2(0,3)
2'	2	1	–2418.791365	0.864869	11.98	–2417.879389	–2417.878445	–2418.010440		2'(2,1)
2''	2	1	–2418.792188	0.864756	13.65	–2417.880306	–2417.879361	–2418.011371		2''(2,1)
6	2	1	–2650.085345	0.974393	8.92	–2649.057547	–2649.056603	–2649.201350		6(2,1)
7a	3	1	–2534.628396	0.929661	12.85	–2533.648024	–2533.647080	–2533.785373		7a(3,1)
7b	3	1	–2534.646426	0.930289	12.52	–2533.665422	–2533.664478	–2533.803237		7b(3,1)
8a-TS	3	1	–2534.627885	0.929123	–160.29	–2533.648520	–2533.647576	–2533.785001		8a-TS(3,1)
8b-TS	3	1	–2534.608917	0.928560	–473.24	–2533.629914	–2533.628969	–2533.766906		8b-TS(3,1)
8a	3	1	–2534.668650	0.930857	11.89	–2533.687118	–2533.686173	–2533.825200		8a(3,1)
8b	3	1	–2534.657907	0.930696	13.57	–2533.676474	–2533.675529	–2533.814741		8b(3,1)
9a	2	1	–2534.433752	0.918991	10.65	–2533.464256	–2533.463312	–2533.602582		9a(2,1)
9b	2	1	–2534.438760	0.919340	10.84	–2533.469055	–2533.468111	–2533.606885		9b(2,1)
MeOH	0	1	–115.670650	0.051924	338.27	–115.615430	–115.614486	–115.641443		MeOH(0,1)
1⊃PTS[i]	–2	1	–5298.710420	1.024668	13.40	–5297.617340	–5297.616396	–5297.790993		1-PTS(-2,1)

[a] Structure code. [b] System charge (n) and multiplicity (m). Optimized geometries are provided as xyz files, named "code(n,m).xyz". [c] Self-consistent field electronic energy. [d] Zero-point vibrational energy. [e] Lowest vibrational frequency. [f] Thermodynamic functions. [g] After annihilation of the first spin contaminant. [h] XYZ file containing the Cartesian coordinates. [i] PCM(H_2O) solvation included.

6. References

(1) Sisto, T. J.; Golder, M. R.; Hirst, E. S.; Jasti, R. Selective Synthesis of Strained [7]Cycloparaphenylene: An Orange-Emitting Fluorophore. *J. Am. Chem. Soc.* **2011**, *133* (40), 15800–15802. https://doi.org/10.1021/ja205606p.

(2) Thordarson, P. Determining Association Constants from Titration Experiments in Supramolecular Chemistry. *Chem. Soc. Rev.* **2011**, *40* (3), 1305–1323. https://doi.org/10.1039/C0CS00062K.

(3) Hibbert, D. B.; Thordarson, P. The Death of the Job Plot, Transparency, Open Science and Online Tools, Uncertainty Estimation Methods and Other Developments in Supramolecular Chemistry Data Analysis. *Chem. Commun.* **2016**, *52* (87), 12792–12805. https://doi.org/10.1039/C6CC03888C.

(4) Bindfit Http://Supramolecular.Org. http://supramolecular.org.

(5) Frisch, M. J.; Trucks, G. W.; Schlegel, H. B.; Scuseria, G. E.; Robb, M. A.; Cheeseman, J. R.; Scalmani, G.; Barone, V.; Petersson, G. A.; Nakatsuji, H.; Li, X.; Caricato, M.; Izmaylov, A. F.; Zheng, G.; Sonnenberg, J. L.; Hada, M.; Ehara, M.; Toyota, K.; Fukuda, R.; Hasegawa, J.; Ishida, M.; Nakajima, T.; Honda, Y.; Kitao, O.; Nakai, H.; Vreven, T.; Montgomery, Jr., J. A.; Peralta, J. E.; Ogliaro, F.; Bearpark, M.; Heyd, J. J.; Brothers, E.; Kudin, K. N.; Staroverov, V. N.; Kobayashi, R.; Normand, J.; Raghavachari, K.; Rendell, A.; Burant, J. C.; Iyengar, S. S.; Tomasi, J.; Cossi, M.; Millam, J. M.; Klene, M.; Adamo, C.; Gomperts, R.; Stratmann, R. E.; Yazyev, O.; Austin, A. J.; Cammi, R.; Pomelli, C.; Ochterski, J. W.; Martin, R. L.; Morokuma, K.; Zakrzewski, V. G.; Voth, G. A.; Salvador, P.; Dannenberg, J. J.; Dapprich, S.; Daniels, A. D.; Farkas, O.; Foresman, J. B.; Fox, D. J. Gaussian 16, Revision B.01, 2016.

(6) Becke, A. D. Density-Functional Exchange-Energy Approximation with Correct Asymptotic Behavior. *Phys. Rev. A* **1988**, *38* (6), 3098–3100.

(7) Becke, A. D. Density-functional Thermochemistry. III. The Role of Exact Exchange. *J. Chem. Phys.* **1993**, *98* (7), 5648–5652. https://doi.org/10.1063/1.464913.

(8) Lee, C.; Yang, W.; Parr, R. G. Development of the Colle-Salvetti Correlation-Energy Formula into a Functional of the Electron Density. *Phys. Rev. B* **1988**, *37* (2), 785–789. https://doi.org/10.1103/PhysRevB.37.785.

(9) Yanai, T.; Tew, D. P.; Handy, N. C. A New Hybrid Exchange–Correlation Functional Using the Coulomb-Attenuating Method (CAM-B3LYP). *Chem. Phys. Lett.* **2004**, *393* (1–3), 51–57. https://doi.org/10.1016/j.cplett.2004.06.011.

(10) Grimme, S.; Ehrlich, S.; Goerigk, L. Effect of the Damping Function in Dispersion Corrected Density Functional Theory. *J. Comput. Chem.* **2011**, *32* (7), 1456–1465. https://doi.org/10.1002/jcc.21759.